UNIVERSITY OF GÄVLE

FACULTY OF ENGINEERING AND SUSTAINABLE DEVELOPMENT
Department of Building Engineering, Energy Systems and Sustainability Science

Photovoltaic Power Plant Aging

Mikel Perez de Larraya Espinosa

May 2020

Publication type, Advanced level (Master degree, one year), 15 HE
Energy Systems
Master Programme in Energy Systems

Supervisor: Björn Karlsson
Assistant supervisor: Mattias Gustafsson
Examiner: Nawzad Mardan

ABSTRACT

One of the most pressing problems nowadays is climate change and global warming. As it name indicates, it is a problem that concerns the whole earth. There is no doubt that the main cause for this to happen is human, and very related to non-renewable carbon-based energy resources. However, technology has evolved, and some alternatives have appeared in the energy conversion sector. Nevertheless, they are relatively young yet.

Since the growth in renewable energies technologies wind power and PV are the ones that have taken the lead. Wind power is a relatively mature technology and even if it still has challenges to overcome the horizon is clear. However, in the PV case the technology is more recent. Even if it is true that PV modules have been used in space applications for more than 60 years, large scale production has not begun until last 10 years. This leaves the uncertainty of how will PV plants and modules age. The author will try to analyse the aging of a specific 63 kWp PV plant located in the roof of a building in Gävle, monitoring production and ambient condition data, to estimate the degradation and the new nominal power of the plant.

It has been found out that the degradation of the system is not considerable. PV modules and solar inverters were studied, and even if there are more elements in the system, those are the principal ones. PV modules suffered a degradation of less than 5%, while solar inverters' efficiency dropped from 95,4% to around 93%.

Key words: Renewable energy, PV system degradation, Potential Induced Degradation (PID), solar inverter.

ACKNOWLEDGEMENTS

In first place I want to thank my supervisor, Björn Karlsson, who proposed this thesis to me. He has helped me with the thesis with several meetings and lots of emails, specially these last weeks. In addition, I also want to thank my assistant supervisor, Mattias Gustafsson. I have been in the power plant with him and also with Mikael Sundberg, who installed all the measurement devices, allowing me to have data for the analysis of the thesis.

I appreciate too the support given by my Erasmus mates, specially the Fanatic Orto Famiglia. Thanks to the collegues in HiG and the people I have known here in Sweden.

Of course, I could not forget my family. They have supported and motivated me to be able to finish the work just on time. Always, since I started studying in school until I am presenting my master thesis at the university. Here I also include my closest ones at home even with the distance and the corona I have been able to keep in touch with them. It has not been easy, but this time is over now and I will be back soon.

TABLE OF CONTENTS

LIST OF FIGURES

LIST OF TABLES

NOMENCLATURE

AC	Alternating Current
C	Capacitor
C_{CM}	Common mode capacitor
C_{DM}	Differential mode capacitor
C_t	Transformer parasite capacitor
DC	Direct Current
EVA	Ethylene-Vinyl Acetate
FF	Fill Factor
G	Solar irradiance
L	Inductance
L_{CM}	Common mode inductance
L_{grid}	Grid inductance
I	Current
I_{CM}	Common mode current
I_D	Diode current
I_L	Photovoltaic effect current
I_{MPP}	Maximum power point current
I_{SC}	Short circuit current
IT	Isolé Terre
MPP	Maximum Power Point
MPPT	Maximum Power Point Tracking
NOCT	Normal Operating Cell Temperature
P	Power
P_{corr}	Temperature corrected power
P_{peak}	Peak power
PID	Potential Induced Degradation
PV	Photovoltaic
R	Resistance
R_P	Parallel resistance
R_S	Series resistance

STC	Standard Test Conditions
T	Temperature
T_{amb}	Ambient temperature
T_{cell}	Cell temperature
TN	Terre Neutre
TT	Terre Terre
V	Voltage
V_{DM}	Differential mode voltage
V_{grid}	Grid voltage
V_{MPP}	Maximum power point voltage
V_{OC}	Open circuit voltage
V_{PV}	Photovoltaic voltage
Z	Impedance
Z_p	Phase impedance
Z_n	Neutral impedance
Θ	Angle of incidence

1. INTRODUCTION

One of the key parts of the development of the society, as we know, is having a stable energy availability. So far, fossil fuels have been the perfect solution for this purpose. Fossil resources have provided a manageable, cost effective and reliable source of energy. However, with the increase of energy use and with the development of the technology, the fact that fossil fuels are not sustainable has appeared. This has led to the research for new energy resources. Renewable energy resources are the solution. Their availability is spread all over the world (unlike fossil fuels), they are ecologically sustainable and, nowadays, they are even more cost effective than traditional fossil fuels.

Even tough renewable resources must face big challenges to become the alternative to fossil fuels, e.g. manageability, nobody doubts that technology will evolve far enough to accomplish this.

The two leading forces of renewable energies are wind power and solar energy. Wind power is a more mature technology than solar energy. Nevertheless, solar energy has grown rapidly during the last 15 years, when the growth rate of PV systems has been of 41%. In addition, it is expected for this growth to continue in the future (Sampaio and González, 2017).

At this moment, solar power is the most cost-effective technology among both fossil fuels and renewable energies, economically and timewise (EIA, 2019). This means that the PV generation technology can be installed and started working significantly faster than traditional technologies, such as combined-cycle, coal or, specially, nuclear plant powers.

However, as is has been mentioned above, PV technology and in general all the new appearing renewable technologies have many challenges to face. These challenges are mainly manageability and integration to the electric grid.

For the PV technology in particular, since it is a rather recent technology, one of its main conundrums is analysing its aging. This is, therefore, the objective of the future research that will be developed with the help of the HiG.

1.1. BACKGROUND

This thesis has been proposed by Björn Karlsson, professor at HiG and Mattias Gustafsson, part time professor at HiG and working in Gävle Energi. The thesis is based on a large PV system installed in the roof of a building owned by Gavlegårdarna, a subsidiary company of Gävle Energy, both companies of the municipality.

It has been considered interesting studying this specific PV system since it is one of the first installed in Gävle. At the time of the installation, 2007, PV power plants were not still economically profitable, and this plant was built thanks to grants to solar energy given by Swedish government. Hereby, it is interesting to see how a plant built at first place which was not economically profitable (without economic support) works after more than 10 years.

1.2. LITERATURE REVIEW

Before beginning the study and analysis of the mentioned PV plant, the author performed a brief literature review to analyse the current information concerned to PV modules and PV systems aging and degradation.

One of the most important factors that degrades the PV modules is the *potential induced degradation*, also known as PID. PID takes place when the module's electric potential is below ground. When the module is subjected to negative potential, positive charges resting inside the glass covering of the module (mainly positive sodium ions) are deposited on the surface of the module decreasing the current output (see Figure 1).

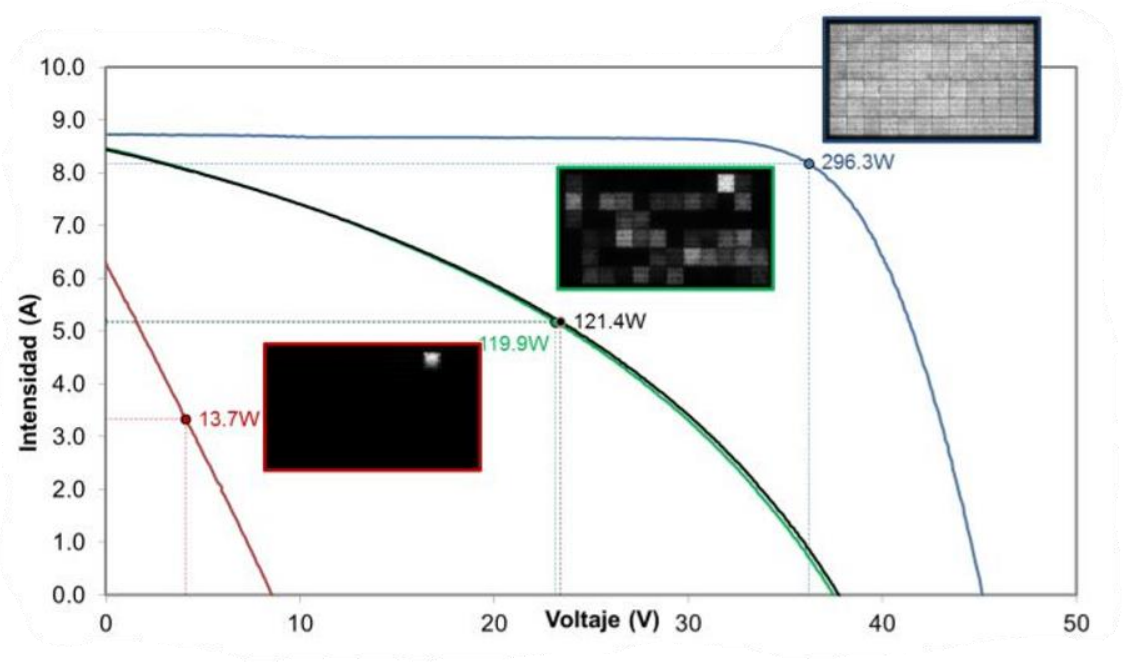

Figure 1: Example of I-V curves after performing a PID test (96h, -1000 V, 60 ºC, 85% R.H.). The original module suffers the degradation from blue I-V curve to green I-v curve and lastly to red I-V curve, with almost no production. (Gonzalez Senosiain, Marroyo and Barrios, 2014).

Many studies and researches analyse the effect of the ambient conditions, e.g. temperature and humidity, (Hoffmann and Koehl, 2014) and of the materials (López-Escalante *et al.*, 2016) on the PID of a PV module. According to these studies, the average value of decrease in Maximum Power Point (MPP) of a PV module is just below 5% when the modules are subjected to a standardized test described by UL certified company. In addition, other paper (Jordan and Kurtz, 2013) reported typical degradation rate in PV modules to be below 5% and being slightly higher in monocrystalline cells than in polycrystalline cells.

Even if this degradation difference is very small, it is worth mentioning that the modules of the studied power plant are made of polycrystalline silicon.

The paper analysing the effect of using different materials as a covering for the PV modules, (López-Escalante *et al.*, 2016), found out that when substituting the traditional Ethylene-Vinyl Acetate (EVA) covering of the module's cells with different polyolefin solutions results improved significantly. This paper showed that when testing a single layer polyolefin covering, the MPP increased by 0,14%, probably due to small inaccuracies in measurements of the results and ambient conditions. For the double layer polyolefin/EVA encapsulation, the MPP decreased by 0,98%. Being this a more substantial change, it is far from the 5% limit mentioned above.

Although this research will not include material analysis, it is very interesting to see how the materials PV cells are made from affect their degradation. All the cells suffer from the same kinds of degradation, however, the effect those processes are very different depending on the construction of the cells.

Another field paper (Liu *et al.*, 2019) compared the aging of two equal PV modules that had been utilized differently. The first of them was used in a PV power plant in California for about 30 years, while the other was stored in a warehouse for the same period. The paper reported a maximum power output shown in Table 1 for the two PV modules.

Table 1: Output power decrease in two different 30-year-old PV modules (Liu *et al.*, 2019).

PV module	Power (W)	Energy loss (%)
Rated power	41	0
Warehouse module	35,9	12,44
Field used module	28,4	30,73

These figures mean that other than usage degradation, a natural degradation also exists in PV modules. Nevertheless, there is a significant difference between the warehouse module and the field used module. According to the paper (Liu *et al.*, 2019), the 59% of output power difference comes from EVA covering degradation. This degradation causes the decrease of the output current of the module, with a similar effect as the PID explained before. The current decrease due to EVA degradation makes sense when related to PID.

The other major power output difference is caused by the resistance of the module. This accounts for the 33% of the power loss. From the 100% total, a 13% is due to the interconnection resistance and the other 20% is because of the cell resistance itself, see R_s in Figure 2.

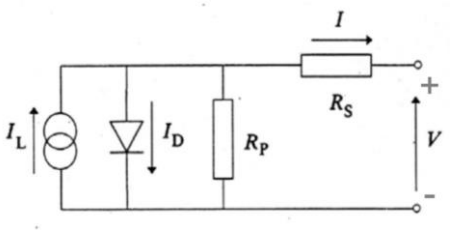

Figure 2: PV cell model of solar modules (Gonzalez Senosiain, Marroyo and Barrios, 2014).

However, it must be considered that this paper (Liu *et al.*, 2019) was performed using more than 30-year-old PV modules. The modules analysed in the paper were produced in 1984. Since then, PV modules have evolved and have been improved, but there is still many information that can be useful.

Despite all of this, it is important to bear in mind that different climates affect very differently to the modules, and the Californian climate is more aggressive for the PV cells than the Swedish climate.

Regarding to the effect the ambient conditions have in the degradation of PV modules, a paper (Omazic *et al.*, 2019) analyses the degradation suffered by different PV modules under 5 different climates. The paper's data has been collected since 1980 and it kept ongoing until it was published in 2019. The most degraded PV modules were the ones in arid or desert climates and in tropical climates. Both climates share a common factor of high temperatures, and this causes EVA degradation and when combined with humidity (tropical climates) corrosion (87% more corrosion in tropical climates than in arid climates).

On the other hand, warm and temperate climates suffer the same kind of degradation but suffer less severe condition, so they can last longer. And the last analysed climate, snow and polar, suffers from different problems. While low temperatures prevent EVA from degrading, low temperatures and snow cause mechanical stress and produce cell cracks, frame breakage or bending and glass breakage.

Given that the author is going to analyse a PV plant located in Gävle, cold climate, it is expected that the deterioration in PV modules will not have a great amount of EVA degradation. However, according to the structural damage of the PV modules, no problem or substitution has been reported.

Other important factor in PV production and damage related to ambient conditions is dust. A paper (Chanchangi *et al.*, 2020) found out that the negative effect dust has in PV modules can vary the power drop from 32% in 8 months (extreme conditions in Saudi Arabia) to just 10% in 18 years with no maintenance (Australia). Considering that with just cleaning it is possible to reduce the effect dust has on PV modules and given that Gävle is not a location prone to suffer dust storms, the negative effect of the dust can be dismissed.

1.3. AIMS

The main aim for this study is to quantify the output power reduction of the whole PV plant since the moment of the installation. This means achieving the understanding on how the energy flows from solar irradiance to AC current. For that purpose, additional measuring devices will be installed (to measure irradiance, temperature, AC and DC electricity output, etc.).

With all the needed tools and information, it will be possible to explain what part of the losses happen in the conversion of energy from irradiance to electricity and how much is lost converting DC current to the final AC current output.

1.4. APPROACH

The aim of the study is to analyse how the system has degraded with time. Therefore, it is logic to have chosen this installation, which was installed in 2008. It is especially important to consider that none of the elements that are part of the whole PV system have been completely changed. This means that no module has been substituted nor any power inverter. It is likely that they may have had some maintenance, but due to the lack of qualified personnel working for the plant, no significant change has been implemented.

The main tasks to achieve for the project development are the following ones:

- Installation of measuring devices. Pyranometer and thermometer linked to an exterior datalogger and wattmeter (current and voltage measures) linked to the indoor datalogger, in inverter room.
- Monitoring the behaviour of the plant for a certain amount of time.
- Comparison of the new data to the old data stored from previous years and to the nominal power of the plant at the moment of the installation.

1.5. LIMITATIONS

The main limitation for the project is the old data stored in the measuring device. Data from 2008 and 2009 is available for the author to have real figures for performing a comparison. However, this data is just daily power production data. Therefore, with the lack of ambient condition information (i.e. irradiation, temperature) or even minutely or hourly data, it is not possible to make a proper comparison.

Hence, one of the solutions considered for the project is to compare daily data from different years taking just the days with greater energy conversion (assuming similar operating conditions at the best point of each year).

Another interesting approach would be measuring and tracking the actual I-V curve of a module (or string) and comparing it to the nominal values of the new modules. Since nominal information of the modules includes an inaccuracy of ±3% even if there may be some error, it is not very significant.

1.6. OBJECT DESCRIPTION

1.6.1. Location and orientation

The studied PV plant is located in Gävle, in the district called Andersberg. Table 2 shows the geographical location parameters of the plant.

Table 2: Geographical location of the PV plant.

Parameter	Value	Orientation
Latitude	60º 39’ 6,3”	N
Longitude	17º 8’ 18,4”	E

To visually facilitate the location of the plant, Figure 3 shows the location of the plant both relative to Sweden and closely in Gävle.

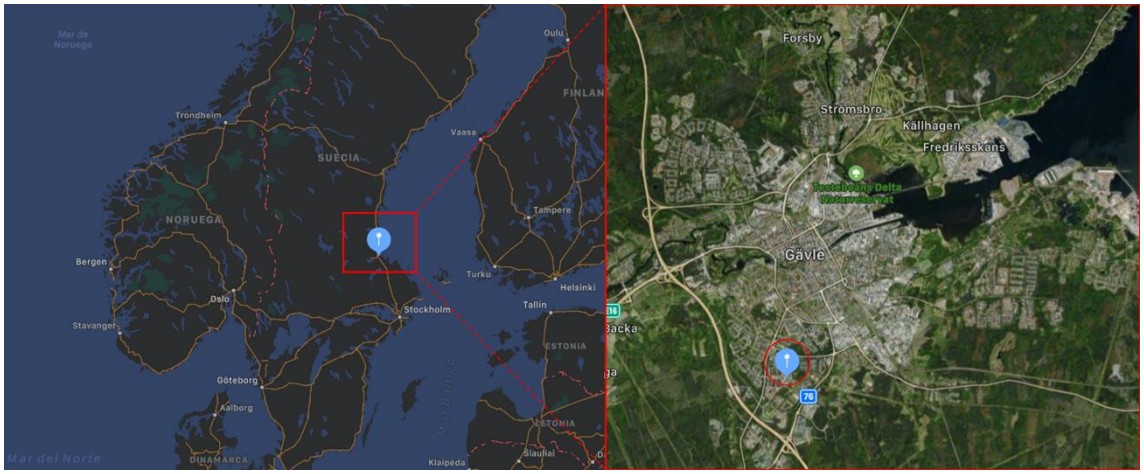

Figure 3: Location of the PV system.

The PV plant is located in the roof of a building owned by Gavlegardarna. The PV modules are divided into 2 sections. The main section, *Part A* in Figure 4, is oriented almost perfectly to the south. Its azimuth angle (γ) is -2,75º. The other section, *Part B* in Figure 4, is oriented facing more to the east, with an azimuth angle (γ) of 42,25º.

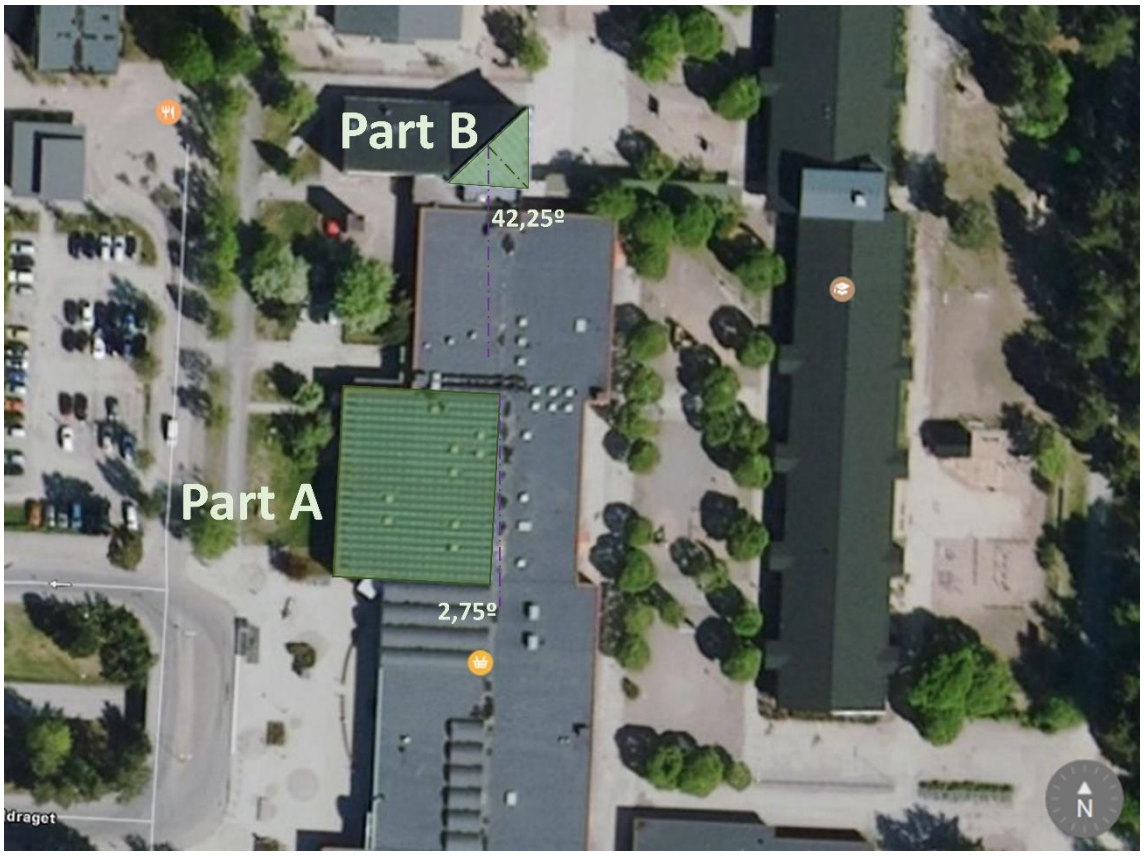

Figure 4: PV plant in the roof of the building. 2 different parts each one with a different orientation.

1.6.2. PV Installation

The PV installation is compound by different elements. The main elements are PV modules and inverters. For being able to work with acceptable voltages, i.e. not too small, PV modules are connected in series to create arrays or strings. Each one of these strings is then connected to an inverter.

1.6.2.1. PV Modules

The PV modules used for this PV plant are NP130GK 13130 Naps polycrystalline silicon modules. Each module is compound by 36 PV cells connected in series, which gives the module an open circuit voltage of 22,1 V. Table 3 shows the specifications of the used PV modules

Table 3: Specifications of the PV modules.

Parameter	Value
Peak power	130 W
Module efficiency	13,1%
Maximum power voltage	17,3 V
Maximum power current	7,5 A
Open circuit voltage	22,1 V
Short circuit current	8,1 A
Power tolerance	±3%
Nominal operating cell temperature	47 ºC ±2%
Cell dimensions	156 x 156 mm

Knowing the temperature coefficients of the PV module is also very important to estimate its behaviour in different ambient conditions. Those coefficients can provide approximations of power and working conditions for different irradiance and temperatures, which is the key to

compare results with different working points. In this case, the coefficients will be assumed approximately to normal values in the literature. See Table 4.

Table 4:Assumed temperature coefficients of the PV modules.

Parameter	Value
Coefficient of short circuit current	0,05%/ºC
Coefficient of open circuit voltage	-0,36%/ºC
Coefficient of maximum power	-0,4%/ºC
Coefficient of maximum power voltage	-0,4%/ºC

1.6.2.2. Strings

In PV plants modules are gathered in series arrays to increase the voltage in the DC side of the inverter. Generally, the higher the voltage of the string the lower the conduction losses will be. Thus, the number of series modules is set by the maximum power the inverter can work with.

The PV plant is compound by 490 PV modules, gathered in 27 strings. The strings are formed by groups of between 20 and 14 PV modules. Table 5 shows how strings are formed.

Table 5: Number of modules per string. Connections to inverters and output AC phases.

Number of modules	Section	Inverter	Tracking	Phase	Peak power (Wp)
19	A	1.1	S1	L1	2470
17	A	1.1	S2	L1	2210
19	A	1.2	S1	L2	2470
17	A	1.2	S2	L2	2210
19	A	1.3	S1	L3	2470
18	A	1.3	S2	L3	2340
19	A	1.4	S1	L1	2470
18	A	1.4	S2	L1	2340
19	A	1.5	S1	L2	2470
16	A	1.5	S2	L2	2080
19	A	1.6	S1	L3	2470
15	A	1.6	S2	L3	1950
19	A	1.7	S1	L1	2470
19	A	1.7	S2	L1	2470
19	A	1.8	S1	L2	2470
19	A	1.8	S2	L2	2470
19	A	1.9	S1	L3	2470
19	A	1.9	S2	L3	2470
19	A	1.1O	S1	L2	2470
19	A	1.1O	S2	L2	2470
16	A	1.11	S1	L3	2080
20	B	2.1	S1	L1	2600
19	B	2.1	S2	L1	2470
20	B	2.2	S1	L2	2600
19	B	2.2	S2	L2	2470
15	B	2.3	S1	L3	1950
14	B	2.3	S2	L3	1820

Figure 5 shows the layout of the plant in the roof. Both parts, A and B, can be distinguished. For the part A of the plant, in the front part of the picture, each row represents a string. It can be noticed in Table 5 that the arrangement of the modules is not done in the same way for all the strings. There are strings of 19 modules (connected to S1 input except in inverter 1.11) and strings between 19 and 15 modules (connected to S2). This rather arbitrary grouping of the modules is due to the layout of the roof.

Figure 5: Modules of the PV plant in the roof of the building. Part A at the front of the picture, Part B in the back-right section, different inclination roof.

The main issue with the layout of the roof is the existence of skylights for inner spaces in the building. They can be seen in Figure 5 as the small white domes in between the modules. When a row of modules is located aside a skylight, a portion of the width of the plant must be left without modules (because of the skylight), therefore, some strings have less modules than others. In addition, this happens to occur every 2 rows of modules, that is why a long string and a short string are connected to each inverter.

1.6.2.3. Inverters

Solar inverters are used to convert the direct current (DC) produced by the PV cells to alternating current (AC). Since almost all devices and grid systems work nowadays with AC, this is a mandatory step. The inverter receives DC power coming from PV modules through the junction box

In addition, inverters are also used to control the output power of the PV plant with MPPT or LPPT algorithms. They try to maximize the output power until it exceeds the nominal power of the inverter (peak DC power is higher than AC power). Besides, it has the function of anti-islanding protection.

The used inverters in the power plant are SMA SB 4200TL HC Multi-string inverters. Their characteristics can be seen in Table 6.

Table 6: Specifications of the inverters of the plant

Parameter	Value
Nominal DC power (W)	4400
Maximum DC voltage (V)	750
MPPT voltage range (V)	125 – 750
Number of inputs	2
Maximum input current (A)	2x11
Maximum output power (W)	4200
Nominal output current	4000
Maximum efficiency (%)	96,2
Euroefficiency (%)	95,4
Number of phases (AC)	1

The peak power the inverters are connected to is up to 15,2% higher than their maximum power. This makes sense with what has been said about higher power in DC side rather than in AC side.

There is a total of 14 inverters, 3 of which are connected each to 2 strings of the part B of the plant. The rest belong to part A. 10 inverters are connected to 2 strings each and the last one is connected to the last string of the plant.

Table 7 shows the peak power of each inverter and the number of modules the inverters are connected to considering both inputs.

Table 7: Inverters with the connected modules and DC power.

Inverter	Modules	Peak power (W)
1.1	36	4680
1.2	36	4680
1.3	37	4810
1.4	37	4810
1.5	35	4550
1.6	34	4420
1.7	38	4940
1.8	38	4940
1.9	38	4940
1.1O	38	4940
1.11	16	2080
2.1	39	5070
2.2	39	5070
2.3	29	3770

Figure 6 shows the inverter room, where all the 14 inverters are located. The inverter room is in the basement of the building, aside the parking.

Figure 6: Inverter room with 14 inverters.

Figure 7 shows a closer look of an individual inverter with 2 inputs. All the inverters but inverter number 1.11 look like this. In Figure 6 a smaller inverter can be seen in the right lower side of the corner (smaller red box). This smaller inverter is the 1.11.

Figure 7: 1.1 inverter in the inverter room.

All the rest of the inverters look like the one in Figure 7. They have the sticker of Naps, which is the manufacturer of the solar panels.

1.6.2.4. Junction box

The junction box measures the current and voltage of each monitored string. This information is then sent to the logger and the output power is calculated. As it has been said, the junction box is between the PV modules and the inverters, therefore, it also has the function of protecting the electrical connections and of being a safety barrier. See Figure 8.

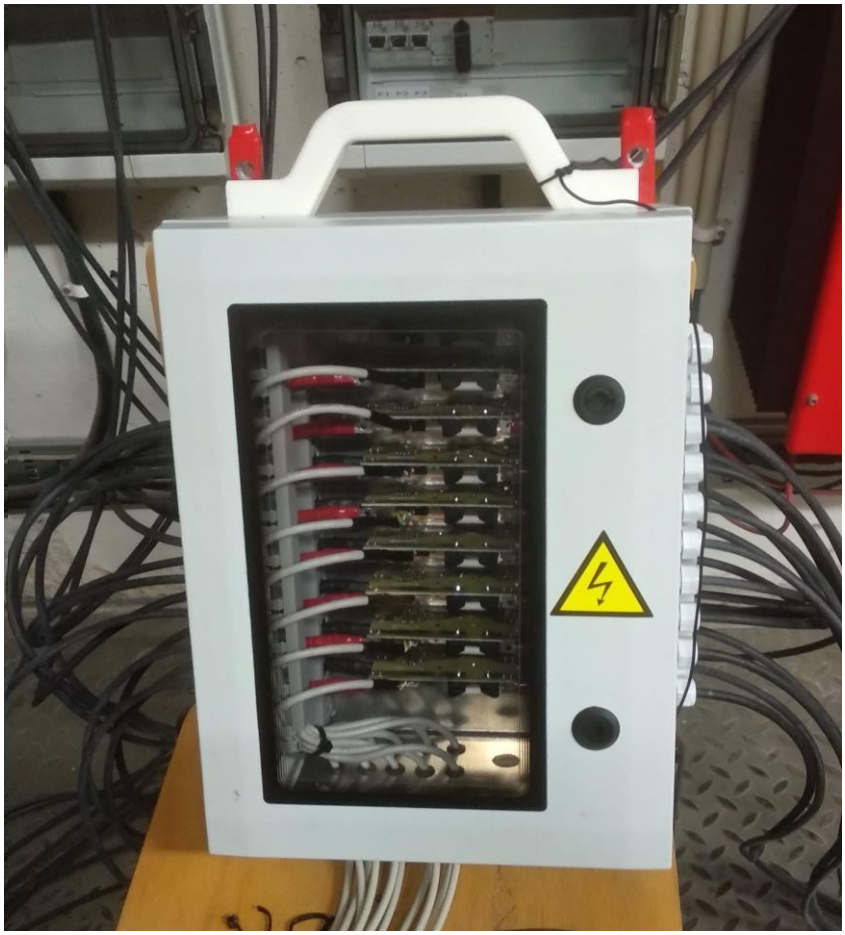

Figure 8: Junction box installed in the inverter room.

2. THEORETICAL BACKGROUND

2.1. SOLAR RADIATION

Solar radiation that reaches the Earth is nature's source of energy for almost every process happening in the Earth. The average amount of energy reaching our planet before entering the atmosphere is estimated to be 1365 W/m^2 (Willson and Mordvinov, 2003). However, due to losses when trespassing the atmosphere (see Figure 9), the maximum irradiation at the surface can be up to 1000 W/m^2 (Chen, 2011). Knowing that the radius of the Earth is approximately $6{,}3781 \cdot 10^6$ meters (Mamajek *et al.*, 2015), the total power reaching the Earth coming from the Sun would be $127{,}8 \cdot 10^{15}$ W. This far exceeds the human energy needs, which were estimated to be $1{,}59 \cdot 10^{14}$ kWh in 2018 (*World Energy Consumption Statistics | Enerdata*, no date).

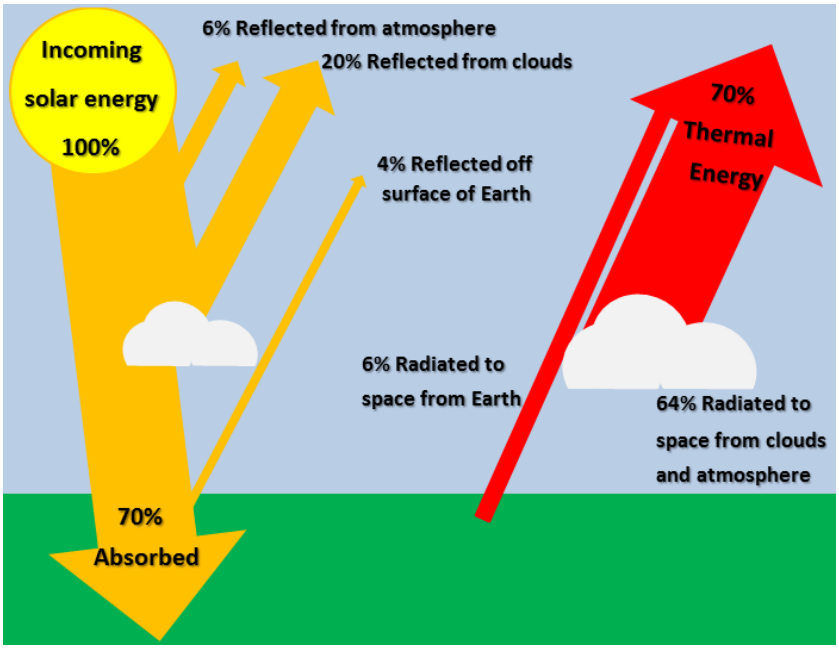

Figure 9: Losses on solar irradiation reaching the Earth's surface.

Therefore, it may seem like solar energy sources are the solution to human energy needs. However, as it is well known, sun power is not manageable, so it cannot meet human needs as the only source of energy. It is, despite all of this, a great choice as an energy production source, if conditions allow it.

2.2. PV SYSTEMS

Photovoltaic (PV) systems are compounded by many different elements. These elements are the ones needed to convert energy from solar irradiance to electricity. Concretely, to AC current, which is the most used way of electricity. AC current is the kind of electricity in the grid too, and, therefore, it is the final step in the energy conversion process.

The system is mainly compounded by photovoltaic cells and inverters. PV cells are the elements that convert solar irradiation to electricity (DC current) through the photovoltaic effect. On the other side, inverters have a double task. Firstly, they are the ones that control the behaviour and the operating point of the PV cells (choosing a point in the given I-V curve). And secondly, they also transform DC current into AC current, more suitable for the usage and for injecting into the electric grid.

PV cell power is measured in peak watts (Wp). This is the power output the PV cell would have when working at Standard Test Conditions (STC), defined in various standards such as UL 1703. STC must meet the following specifications:

- 1000 W/m^2 solar irradiance,
- Cell temperature 25ºC.

At those conditions, the output power of the PV cell is called the peak power, measured in Wp.

2.3. MODULE DEGRADATION

Since PV cells do not have moving parts, solar modules use to be very robust and reliable. That is why they can continue working after decades with minimal maintenance. However, PV modules also suffer from some kinds of degradation.

The main type of degradation suffered by the solar cells that reduces their output power is *Potential Induced Degradation*, also known as PID. The effect of PID has been analysed in LITERATURE REVIEW, but now, a more in dept explanation is going to be given about the process.

PID has two components. A reversible one, due to the polarization of the module cell and an irreversible one, due to the corrosion of the cell itself in the EVA-glass interface. The materials that PV modules are made from are very related to the degradation level PID will produce to the cells, since corrosion tendency and positive ion availability can vary significantly amid different materials. Moreover, ambient conditions, e.g. humidity, can also affect and accelerate the process. This material dependency is the reason because of many researches are performed related to this topic.

PID happens naturally when not connecting any point of the PV string to ground potential. In that case, the middle modules take approximately ground potential and the modules above have positive potential while the ones below the middle modules have negative potential and suffer the PID.

However, PID happens just when the modules are receiving solar irradiance, i.e. when daylight is available. Therefore, at night the reversible effect can be reverted externally applying a positive potential to the modules. This is, nevertheless, an expensive solution and is usually substituted by connecting the first module of the array to ground potential. Although connecting the first modules has the drawback of requiring greater electric insulation in module frames, it is the most common solution (González *et al.*, 2008).

However, connecting the beginning of the string causes another great problem too. Even if it is useful to prevent PID from happening, there is the problem that a ground circuit could be closed. This depends on the type of grounding system used by the grid to which the inverter is connected. The problem is common mode currents circulating through earth (Gubía *et al.*, 2007).

If the grid is isolated from the ground (IT connection), then there is no problem in connecting the beginning of the string to earth. However, if the grid is connected to earth (TT or any type of TN), then, the circuit through earth will be closed, allowing ground currents to circulate (see Figure 10).

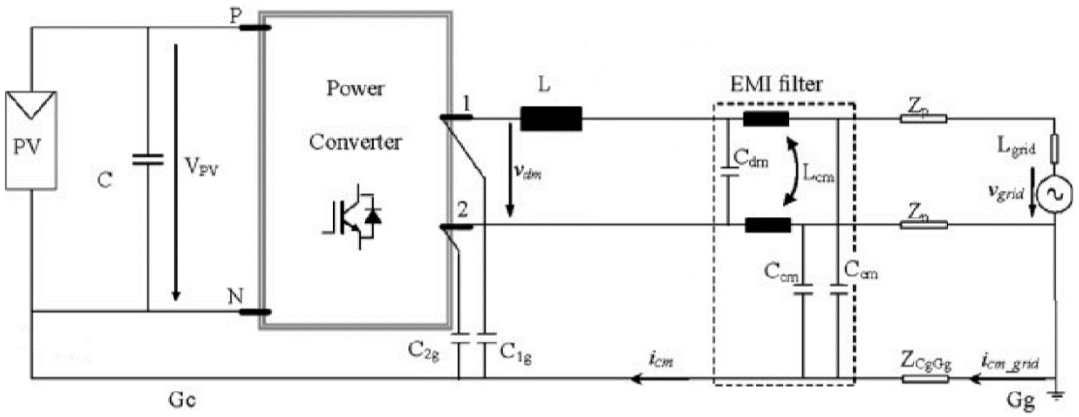

Figure 10: PV system model with TN or TT grid and connection of the beginning of the string to earth to prevent PID. Common mode current can circulate through earth.

If the grid is isolated from earth common mode currents would not be able to circulate.

To prevent currents from circulating in a system connected like the one in Figure 10, galvanic insulation is needed somewhere in between the PV system and the grid. A transformer can be used for this purpose, however, magnetic losses will appear and decrease the total efficiency of the system (see Figure 11).

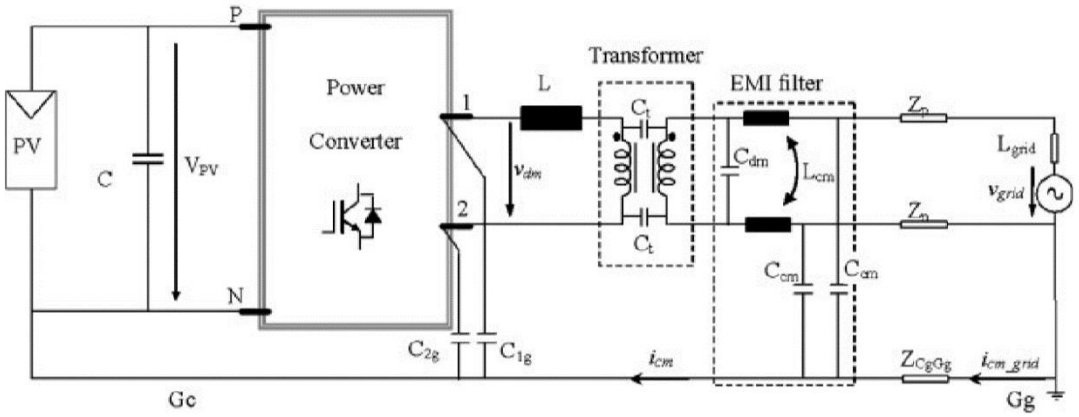

Figure 11: PV system model with TN or TT grid and connection of the beginning of the string to earth to prevent PID. With a transformer, common mode current can circulate through earth.

It is impossible to fully avoid common mode currents. However, serial capacitors like the ones modelling the transformer reduce those currents by various orders of magnitude, downsizing the problem by the same measure.

Transformerless inverter technologies take advantage of DC voltage not being able to go through parasite capacitors, like the ones between earth and PV modules in solar power plants. In this case, nevertheless, the parasite capacitor is being short-circuited to prevent PID. This makes transformerless inverters unable to fully avoid ground currents if the grid is connected to earth (González *et al.*, 2008).

To sum up, even if PID can lead to very severe PV cell damage, the solution is relatively easy to adopt. There is, however, the drawback of ground currents in the PV system, therefore, filters would be required to reduce this current. Preventing PID entails other problems, so the solution adopted by the studied power plant will have to be closely looked at (González *et al.*, 2007).

2.4. I-V CURVE

The behaviour of a photovoltaic cell is defined by its I-V curve, also called current-voltage curve. This curve gives the relation between the output current and the output voltage available under some ambient conditions (i.e. irradiance and temperature). The I-V curve is measured experimentally, usually under STC (*standard test conditions*, solar irradiance 1000 W/m^2 and cell temperature 25 ºC).

The measurements are taken varying the output voltage from 0 to its maximum, which can be achieved changing the external resistance from 0 to infinity. Then, interpolating the points, the characteristic curve is formed.

Similarly, the P-V curve also gives information about the relation, in this case, between the power and the voltage of the cell. The P-V curve can be obtained from the I-V curve just multiplying the current with the voltage. Figure 12 shows a typical I-V and P-V curve of a PV cell.

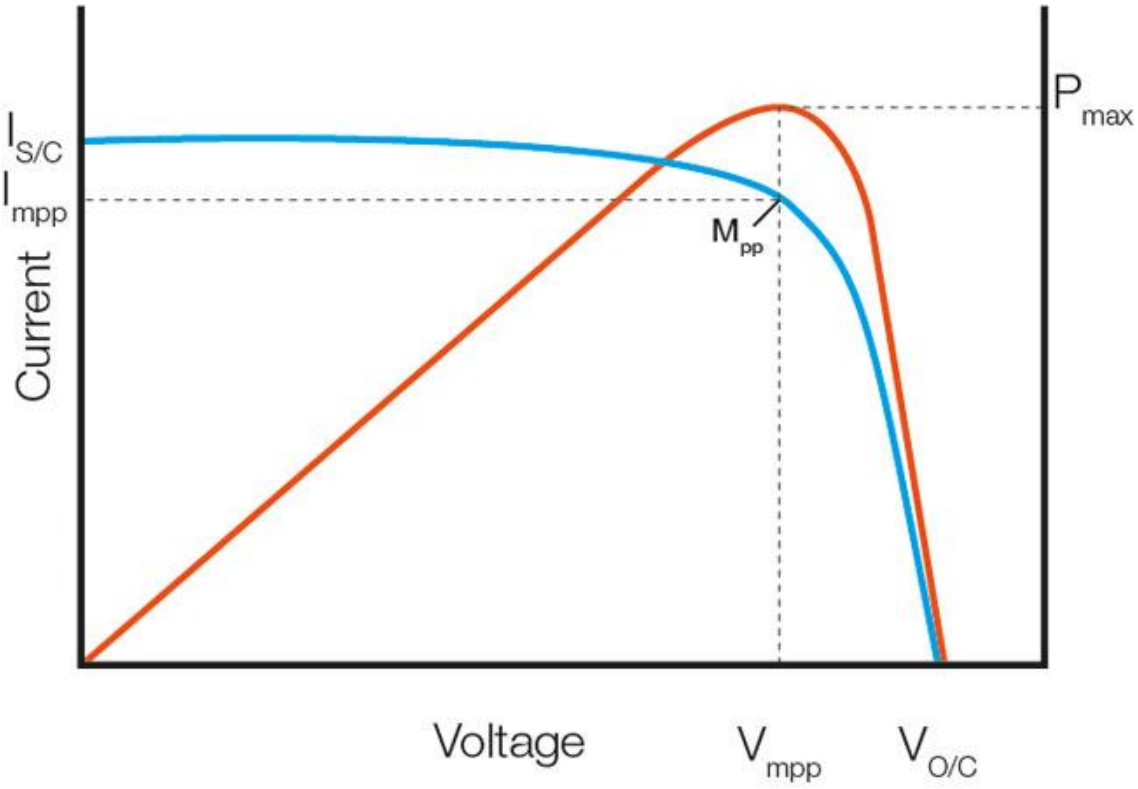

Figure 12: I-V and P-V curves of a photovoltaic cell (*Curve Tracing FAQ's | Seaward Group USA*, no date)

The equation of the I-V curve is shown below (Wang *et al.*, 2007),

$$I_{out} = I_L - I_0 \cdot (e^{\frac{q \cdot V_{out}}{n \cdot k \cdot T}} - 1)$$

Where,

- I_{out}: output current [A],
- I_L: current generated by the photovoltaic effect [A],
- I_0: saturation current of the parallel diode [A],
- *e*: Euler's number,
- q: charge of an electron [C],
- V_{out}: output voltage [V],

- n: diode ideality factor,
- k: Boltzmann's constant [J/K],
- T: cell temperature [K].

Three main important points can be defined in the I-V curve of a solar cell. First of all, when the voltage is 0 (low output impedance) the current is defined as the short circuit current (I_{SC}). This current is the maximum output current value that PV cell can provide. In an ideal solar cell this would be the output current in operation. Nevertheless, due to parallel diode, when increasing the voltage (and very dependant on temperature) the output current is reduced from the I_{SC} value (*IV Curve | PVEducation*, no date).

Secondly, when the output impedance is close to infinity, i.e. when the output current is 0, the voltage provided by the PV cell is called open circuit voltage (V_{OC}). Similarly to what happened with the I_{SC}, V_{OC} is the maximum voltage difference the cell can deliver (*IV Curve | PVEducation*, no date).

As in every electric device, the power can be calculated multiplying the output voltage and the current for the cell.

$$P = I \cdot V$$

Even if short circuit current and open circuit are the maximum output values for both current and voltage, since they are given while the other parameter is 0, the provided power is 0 in both cases. This leads to the third important point when defining the I-V curve of a cell. This point is the maximum power point (MPP), where current and voltage take the values I_{MPP} and V_{MPP}, respectively.

To determine the quality of a photovoltaic cell, the fill factor (FF) is used (see Figure 13). The FF is the ratio between the power of the solar cell and the ideal maximum power calculated from I_{SC} and V_{OC}.

$$FF = \frac{I_{MPP} \cdot V_{MPP}}{I_{SC} \cdot V_{OC}}$$

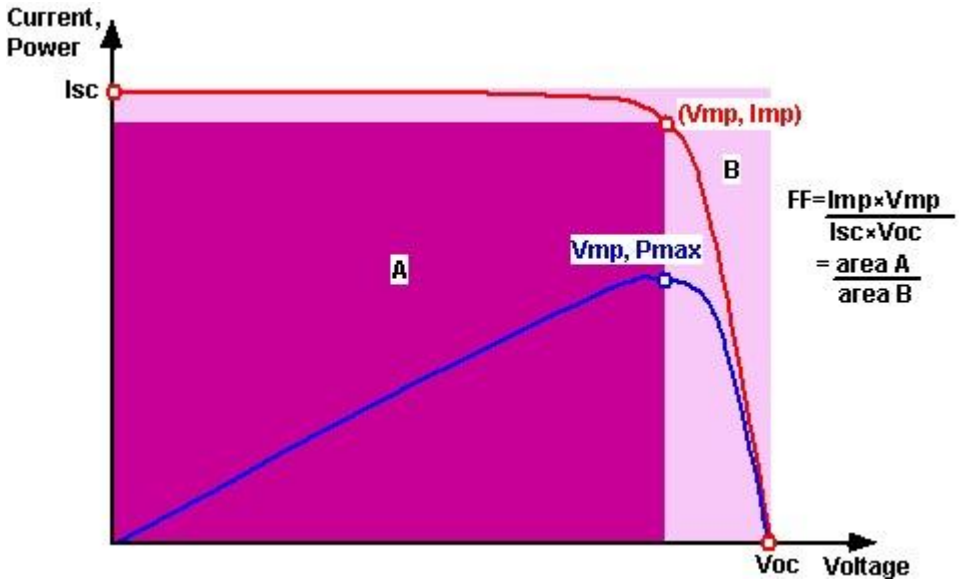

Figure 13: Fill factor represented among I-V and P-V curves (*Fill Factor | PVEducation*, no date).

2.5. EFECT OF IRRADIANCE AND TEMPERATURE

Solar cells are characterized by testing them at STC. However, they rarely operate at STC. As it has been explained before, PV cells have a behaviour very dependant on irradiance and temperature. This is what is going to be explained in this subsection.

Even if both external conditions, i.e. irradiance and temperature, have effect in both outputs of a PV cell, i.e. current and voltage, to simplify the explanation it is going to be assumed that each factor will have effect in just one output parameter. This is not a bad approximation, as it is going to be showed.

Irradiance can vary in a range from 0 to 1000 W/m^2 and its intensity is proportional to the output current of the solar cell. Since the output current is affected by the diode conductivity, this proportional relation can be seen in the I_{SC}, when the output voltage is 0. Figure 14 shows how the I-V curve changes depending on the available irradiance. Notice that, as mentioned before, V_{OC} changes too, but the main effect is seen on the output current, so this effect can be dismissed (Cuce, Cuce and Bali, 2013).

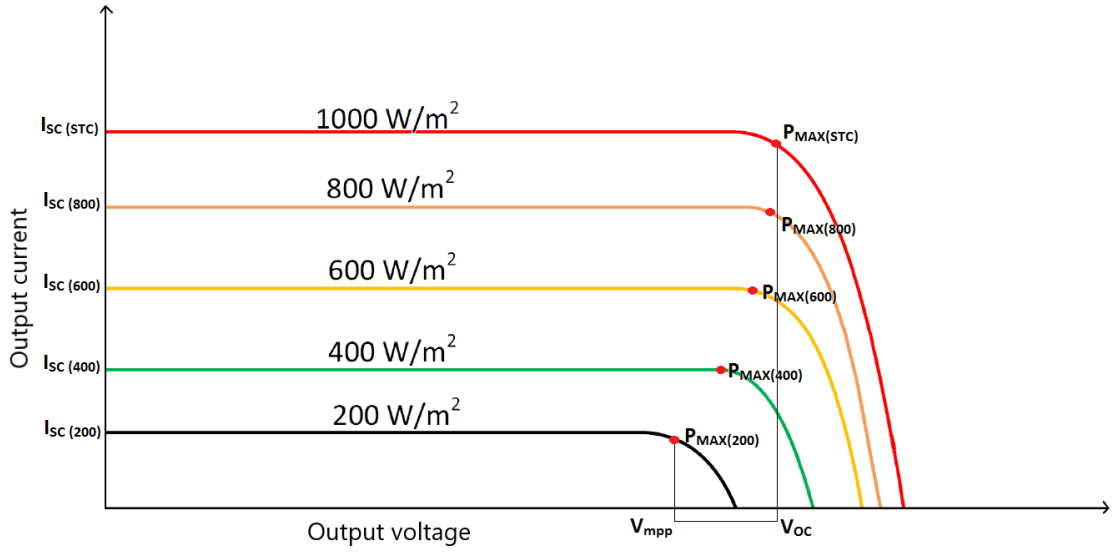

Figure 14: Variation of the I-V curve with different irradiances(Influencia de la irradiación y temperatura sobre una placa fotovoltaica « Ingelibre, no date).

Note that the effect temperature has in the I-V curve is not an effect of just the ambient temperature. Instead, the ultimate effect of the temperature is seen through cell temperature. This means that even if ambient temperature has an effect, it is shared with windspeed, humidity and solar irradiance.

When solar irradiance is high there is more energy available for converting into heat through losses. Some part of the heat is retained and it increases the temperature of the PV cell.

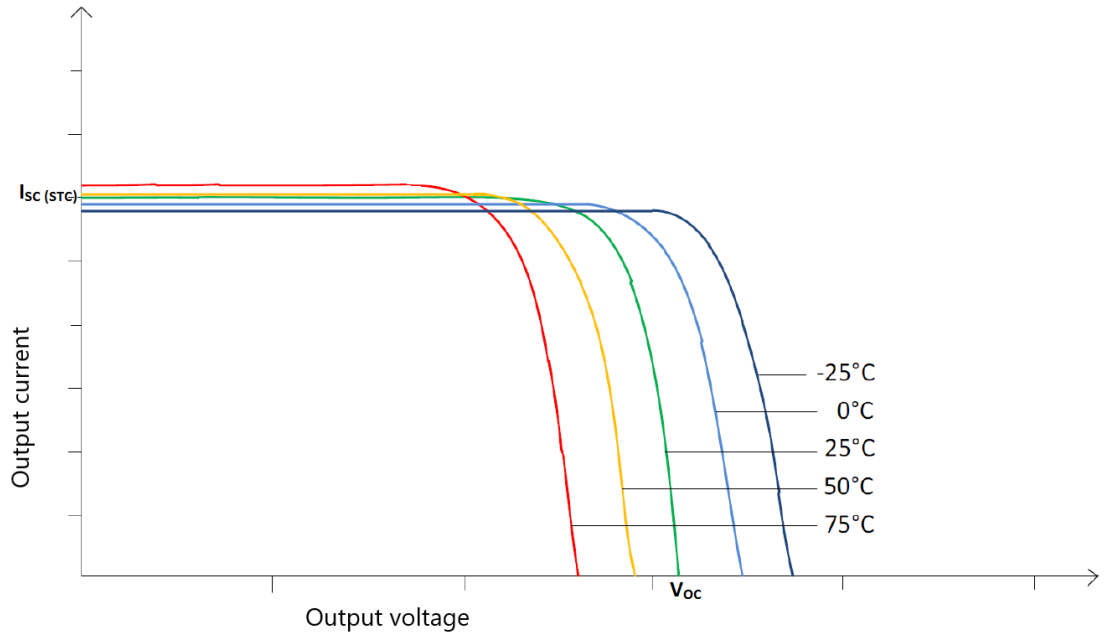

Figure 15: Variation of the I-V curve with different cell temperatures (*Influencia de la irradiación y temperatura sobre una placa fotovoltaica « Ingelibre*, no date).

The effect of temperature in the performance of the solar cell is mostly noticed in the output voltage (see Figure 15). This is due to the fact that for higher temperatures the parallel diode starts conducting current more easily. Therefore, it has a lower conducting voltage. Another way of explaining this is that when temperature is increased, the bandgap energy of the silicon decreases. On the contrary, this better conducting effect also affects having a lower output resistance, hence, I_{SC} increases slightly, but once again, this effect can be dismissed (Zaoui *et al.*, 2015).

As it is shown in Figure 16, the increase of I_{SC} cannot be noticed in the P-V curve of the cell. Therefore, the power will be reduced as the temperature increases.

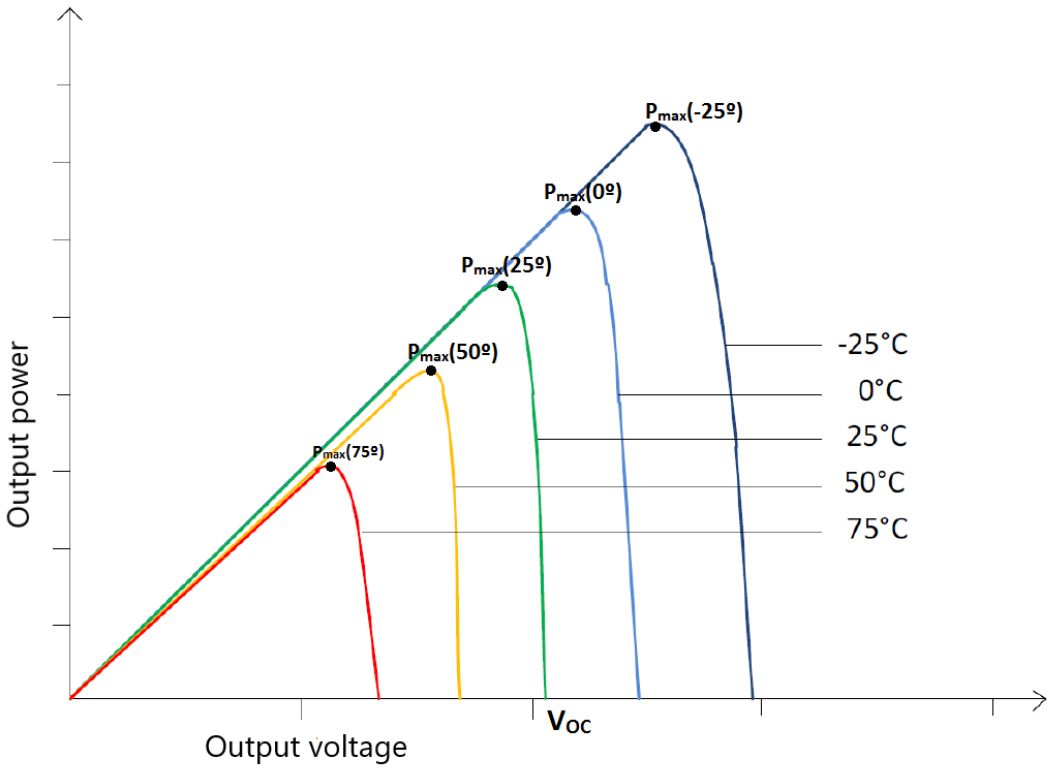

Figure 16: Variation of the P-V curve with different cell temperatures (Influencia de la irradiación y temperatura sobre una placa fotovoltaica « Ingelibre, no date).

All in all, if the other parameter remains constant, maximum power point will increase when solar irradiance increases (proportionally) or when cell temperature decreases.

2.6. SHADING

Since PV systems generate electricity thanks to sunlight, shadows coming from clouds trees or surrounding elements (e.g. buildings) negatively affect the performance of the PV plant (Silvestre and Chouder, 2008). However, the importance of shadowing in PV generators does not come from the reduction of the total irradiance received by the solar cells. Instead, it comes from the difference of irradiance received by different PV cells that are part of the same string.

When the PV modules are connected in series along a string, the common working point for all the modules in that string is the output current. Thus, the module producing less current will restrict the current of the string, causing the reduction of performance of the whole string (Woyte, Nijs and Belmans, 2003).

It is known that output current and irradiation are closely related, therefore, with the partial shadowing of just one module, if no additional measures are taken, the effect will be the same as if all the string was under the low irradiation conditions.

If the current is not restricted by the lower current cell, the shaded cells could work in reverse bias. In reverse bias the cells behave like resistive loads instead of generators. Since they are consuming energy, it is transformed into heat creating hotspots. These hotspots can lead to irreversible damage in the cell (Silvestre and Chouder, 2008).

Nevertheless, to protect the cells, it is possible to install bypass diodes in parallel with the solar cells so that the current will be bypassed in case of a partial shading. When there are no shaded cells, the diodes are blocked and the current flows through the cell. However, if a partial shade

appears, the bypass diode will start to conduct the current produced by the rest of the PV cells (Rodrigo, Gutiérrez and Guerrero, 2015).

Figure 17 shows the schema of how the bypass diode is installed in parallel with the solar cells. If the diode starts conducting current, then the corresponding PV cell will not generate any electricity, but it will be protected from working in the reverse bias zone.

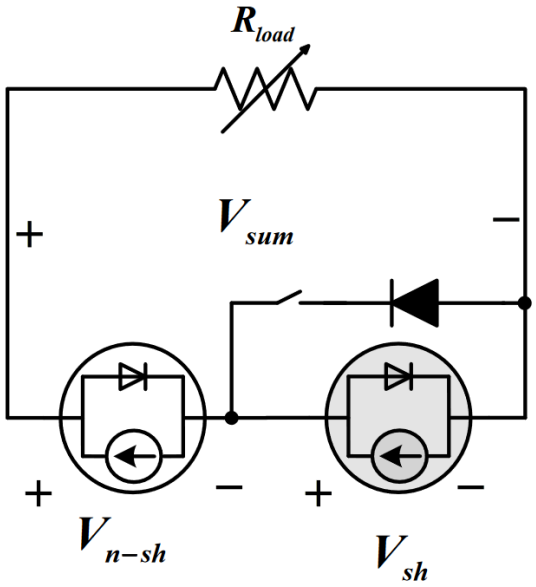

Figure 17: Two PV cells with different irradiance intensities connected in series (with and without bypass diode in parallel with shaded cell) (Sera and Baghzouz, 2008).

Figure 18 shows the I-V curve of the schema shown in Figure 17, where there are two solar cells connected in series and one of them receives less solar irradiance. The chart shows all 4 combinations of I-V curves: cells alone and with and without bypass diodes.

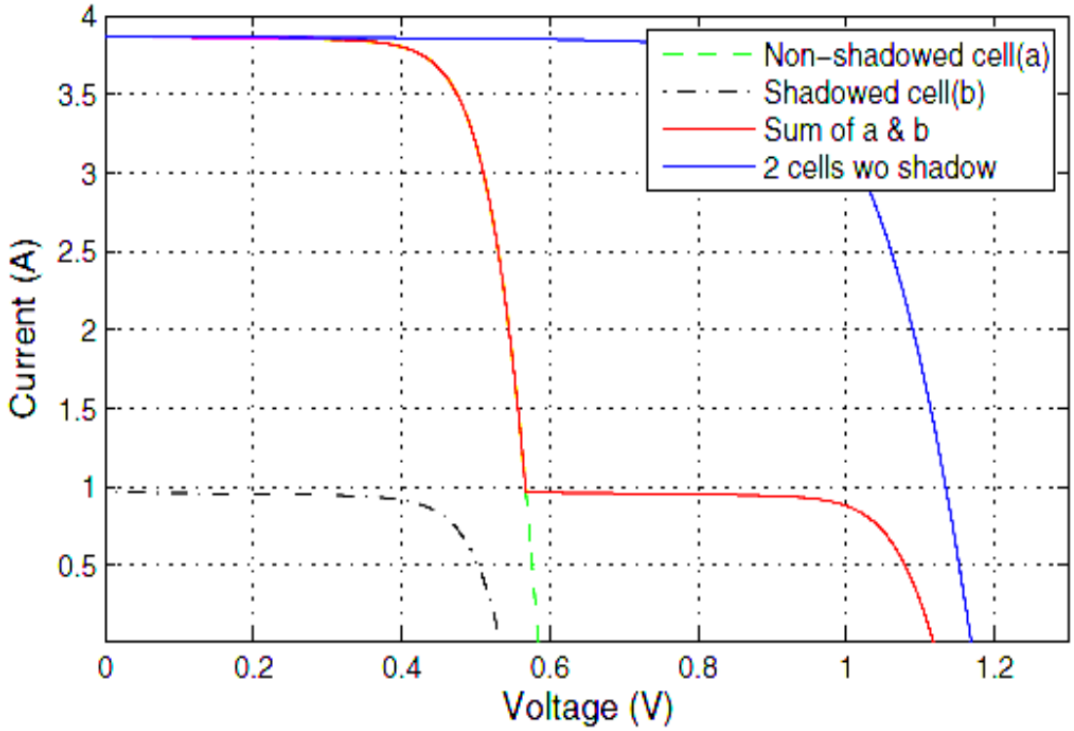

Figure 18: I-V characteristics of two PV cells connected in series with different solar irradiance intensities (Sera and Baghzouz, 2008).

Figure 19 shows the P-V curve for the two cells explained above. Even if the cells are protected with the diode, the reduction of the output power is still a problem. In addition, since the diodes change substantially the behaviour of the system as a whole (including both cells), the P-V curve has local and global maximums. This means that the MPPT algorithm will have to be much more complex to track properly the MPP in shading situations.

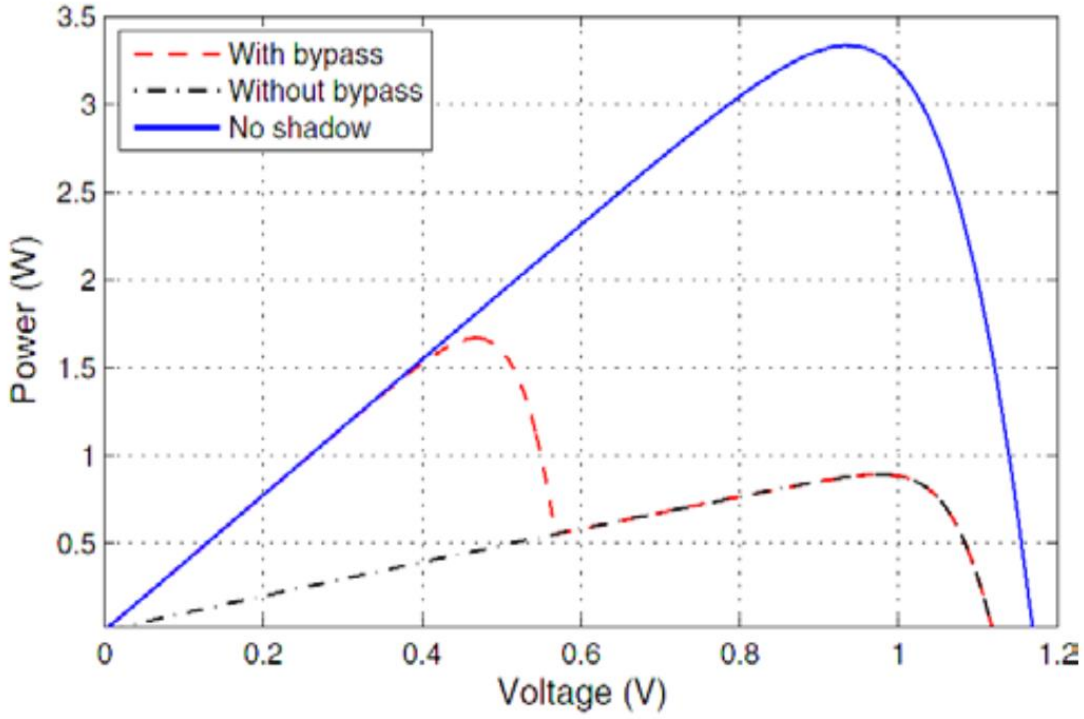

Figure 19: P-V characteristics of two PV cells connected in series with different solar irradiance intensities (Sera and Baghzouz, 2008).

To sum up, bypass diodes can protect properly the individual cells of a PV string (where cells are connected in series). However, there is still a significant reduction of output power due to irradiation decrease. Also, the P-V curve is more complex and, therefore, the MPPT algorithm must be too. Moreover, installing bypass diodes entails other problems such as more expensive modules or losses in the diodes but this is the solution the PV industry has finally adopted.

3. METHODS

Along the Method chapter, an in-depth explanation of the analysed PV plant and the followed procedures to obtain results will be explained. Firstly, the description of physical equipment is going to be done. Later, what calculations and how they are carried out will be explained, so that the results are relevant.

3.1. MONITORING SYSTEM

Considering that solar power is not a constant source of energy and that it drastically depends on external conditions, it is essential to monitor those ambient conditions to understand the results. The monitored parameters are temperature and light irradiation.

The used devices are:

- Ambient temperature sensor,
- Reference solar cell,
- Pyranometer,
- Photodiode.

Not all of them are essential, the pyranometer and the reference solar cell have both the purpose of measuring the irradiance. However, since the university has these resources it has been considered adequate to install all the devices to have more information available. Figure 20 shows the monitoring platform, compound by all 3 sensors.

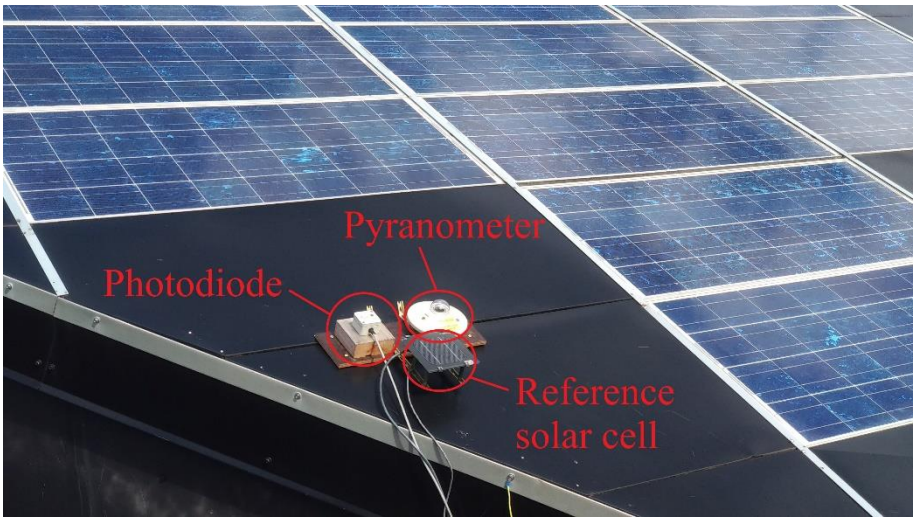

Figure 20: Monitoring system on the roof of the building. Compound by reference solar cell, pyranometer and photodiode.

3.1.1. Ambient temperature sensor

The temperature sensor is used to obtain the ambient temperature, not the cell temperature. Therefore, then this measure will have to be transformed to obtain the cell temperature, which is the parameter directly related to PV cell operating conditions.

The temperature sensor is enclosed in a casing to protect the equipment from external factors such as solar irradiance and water. To avoid affecting the measurements, the casing has several holes that allow the airflow. Hereby, the measured temperature will be the air temperature.

The sensor type is a PT-100, which is located closer to the logger room in the roof than the rest of the equipment, which is in the roof where the PV modules are. However, since air temperature does not vary within the distance the sensor is located, the measurements are assumed as reliable for ambient temperature.

3.1.2. Reference solar cell

The reference solar cell is a monocrystalline PV silicon cell. It is actually formed by 2 independent PV cells. One has the purpose of measuring the irradiance via short circuit current and the other monitors the temperature via open circuit voltage.

The cell measuring irradiance is connected to a very small resistance where the short circuit current is measured as a voltage. The voltage is proportional to the solar radiation. The cell measuring cell temperature is left in open circuit to measure the voltage. The technical specifications of the reference solar cell are shown in Table 8.

Table 8: Technical specifications of the reference solar cell (Lundqvist, Helmke and Ossenbrink, 1997)

Short circuit current signal	28,7 mV per 1000W/m^2
Alpha (α)	0,007 mV/ºC
Open circuit voltage signa	586,7 mV per 1000W/m^2
Beta (β)	-2,17 mV/ºC
D	33,11 mV

See Figure 20 shows the arrangement of the sensors on the roof.

3.1.3. Pyranometer

A pyranometer is a measuring device which detects direct and diffuse solar radiation on a flat surface. The sensor gives a voltage signal: 13,11 mV when the solar irradiance is 1000 W/m^2. See Figure 20.

3.1.4. Photodiode

The measuring platform integrates a photodiode developed by previous year students in HiG and Björn Karlsson. Taking advantage of this, there is another source of information if needed. However, since the reference solar cell and the pyranometer work properly and have higher precision, the photodiode is not used to measure irradiance. See Figure 20.

3.1.5. Logger

Once the sensors have been described, the device used to record those measurements is a data logger. The base of the logger is a digital processor, which works with voltage inputs. The loggers must work connected to a computer, to be able to store the data correctly. Therefore, a laptop was left connected to each logger.

Three loggers have been used to monitor the measurements. For the ambient conditions, i.e. the signal coming from the pyranometer and from the reference solar cell one special location had to be found. Sheltered from the outside but close to the roof. This logger and the laptop are in a room with direct access to the roof. The used logger is Agilent 34970A. See Figure 21.

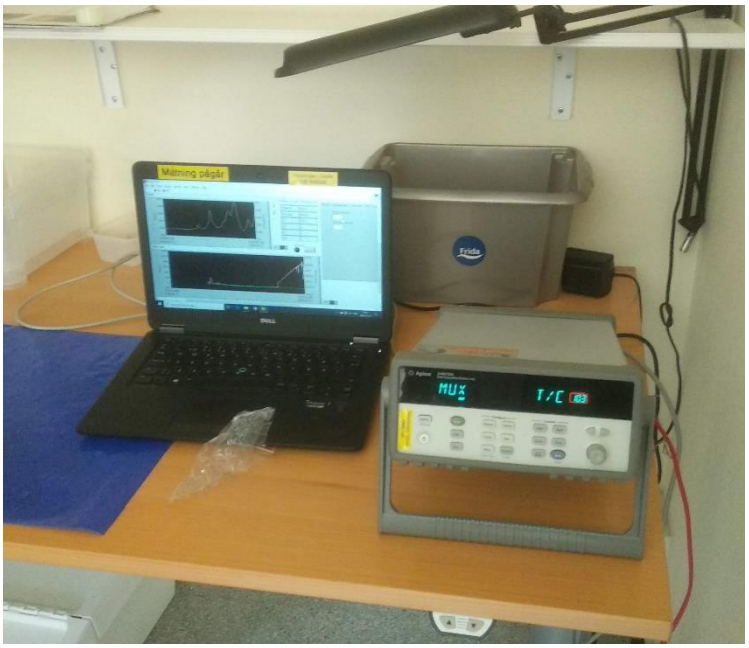

Figure 21: Data logger in the room with direct access to the roof.

The rest of the measurements are performed in the inverter room. Thus, the loggers are located there. Another Agilent 34970A logger is used to monitor the power, current and voltage measurements in the DC side of the installation. This logger is, again, connected to another laptop in the inverter room. See Figure 22.

Lastly, a Fluke logger is used to track the power measurements in the AC side of one of the inverters. This logger does not need from a computer to properly work; therefore, it is an independent measuring system.

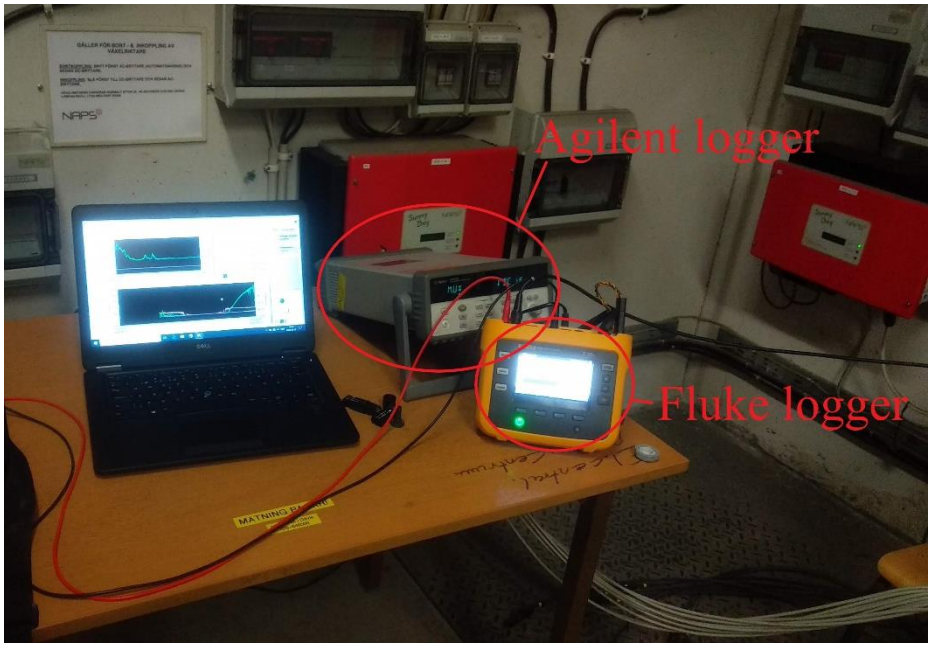

Figure 22: Data loggers in the inverter room for power measurement.

The recording time is equal for all three loggers. They save data every 5 seconds for all signals, including ambient conditions, DC electrical variables and AC electrical output.

3.2. DATA ACQUISITION

The data is stored in the logger until the logger is connected to the computer to get the data. To transfer the information from the logger to the computer a specific software is used. The utilized software is LabVIEW (Laboratory Virtual Instrument Engineering Workbench), from National Instruments, for the Agilent loggers.

For the Fluke logger, the process is easier, since the devices allows to transfer the data directly to a USB memory, to then transfer it to a computer, where is going to be analysed.

3.3. OBTAINING RESULTS

Once the data is acquired from the logger through LabVIEW or to the USB memory, some transformations must be done to convert that raw data into useful information. For that purpose, the used software Microsoft Excel, which allows repeating the same operations to a great amount of data with minimum time waste.

The data obtained with the loggers is recorded every 5 seconds. This data will be used, however, in order to homogenize the recorded information, a minutely average is calculated. The following calculations and results are obtained from those minutely average values.

The main idea is to find a relation between the output power of the PV system and the ambient conditions it is working on. Then, with that relation, an extrapolation will be performed to see if under STC the results match (probably not) the nominal power in the datasheet. Then, a study on the degradation will be performed.

3.3.1. Real power

As it has been said, the junction box measures current and voltage of 4 strings entering 2 of the inverters (DC). Then, the output of one of the inverters is measured again (AC). Having the current and the voltage, it is easy to calculate the power in the DC side with the Equation 1.

$$P(W) = I \cdot V \tag{1}$$

However, this gives the power of the string in the DC side. It is not a problem, but the number of PV modules will have to be considered, and they will not be studied separately, but gathered in strings.

For calculating the power of the AC side (inverter output), the voltage and the current are also needed, but in this case, their relative phase is important too, see Equation 2.

$$P(W) = I \cdot V \cdot cos\varphi \tag{2}$$

It can happen that the inverter is injecting reactive power to lift the voltage, or that it is consuming reactive power. The phase depends on the functioning mode of the inverter, since it is not known, it is easier to measure the phase and then calculate the active power.

3.3.2. Corrected power

The corrected power refers to the power in the DC side. When recording the data of the output and of the ambient conditions it is important to assure that the measured values give useful information. To do so, some transformations must be made regarding to the irradiance and to the measured temperature. For example, the irradiance received by the PV modules can be different in the same conditions depending on the angle of incidence. In that case, a transformation to the measured irradiance would have to be made, see Equation 3.

$$P_{corr}(W) = k(T) \cdot k(\theta) \cdot P \tag{3}$$

Where *k(T)* and *k(θ)* are corrections of the measured power according to temperature and angle of incidence, respectively.

In this particular case, corrections on the measured irradiance are not needed, since instead of using the pyranometer to measure irradiance, the used device was the reference solar cell. As the reference solar cell is placed with the same angle of incidence as the PV modules in the measured strings, this transformation is not needed. For the equation 3, the *k(θ)* term has a value of 1.

However, for the measured temperature corrections must be made. Even if the reference solar cell's open circuit voltage is closely related to ambient temperature it does not give the temperature of the PV cells of the plant. Once the ambient temperature has been measured, the values in the datasheet of the PV modules are then used to correct the measurements. With this process it is possible to estimate the cell temperature using the reference solar cell.

This is because ambient temperature is a global parameter, which affects equally to all equipment, whereas cell temperature in the reference solar cell is specific to that kind of cell, which is different to the PV modules of the plant. In addition, in the reference solar cell, there is no circulating current (measuring open circuit voltage can have current but not significant), therefore, the operating conditions of the PV modules and of the reference solar cell are not the same and corrections would have to be made.

Therefore, the term *k(T)* of the equation 3 will have to be calculated. The process is explained below.

3.3.2.1. Irradiance

As it has been mentioned before, among the 2 ways of calculating solar radiations the reference solar cell has been chosen for more simplicity. With the reference solar cell, a voltage signal referring to the short circuit current of the cell is received, this voltage signal depends on the parameters showed in Table 8. Equation 4 shows how the irradiance is calculated based on those parameters.

In addition, previous works using this measuring device (Júlia Solanes Bosch, 2017) considered that when measuring irradiance with the reference solar cell, a correction factor of 1,02 had to be used.

$$Irradiance_{RSC}\left(\frac{W}{m^2}\right) = 1{,}02 \cdot \frac{V_{Isc}}{28{,}7/1000} \tag{4}$$

Where V_{ISC} is the tension signal obtained from the reference solar cell relative to the short circuit current.

Even if the measurements of the pyranometer are not used, it is worthy showing how the calculations for the irradiation would be made, in a very similar way to the reference solar cell explained above, see Equation 5.

$$Irradiance_{pyr}\left(\frac{W}{m^2}\right) = \frac{V_{pyr}}{13{,}11/1000} \tag{5}$$

Where V_{pyr} is the tension signal obtained from the pyranometer relative to the measured irradiance.

3.3.2.2. Temperature of the cells

It has been mentioned above why the temperature is going to be calculated form the ambient temperature sensor and not from the reference solar cell as it happens with the irradiance. The

reason is simplicity. It is easier to correct the measurements of ambient temperature than correcting the measurements of a reference solar cell which is in a different working point from the PV modules.

To correct the temperature measurements and to obtain cell temperature instead of ambient temperature Equation 6 is used.

$$T_{cell} = T_{amb} + (NOCT - 20) \cdot \frac{G}{800} \quad (6)$$

Where:

- T_{cell}: Temperature of the PV cells of the plant [ºC],
- T_{amb}: Ambient temperature measured by the ambient temperature sensor [ºC],
- NOCT: Normal operation cell temperature [ºC],
- G: Solar irradiance [W/m^2].

The NOCT value is given in the datasheet of the PV modules. It is defined as the cell temperature under the following ambient conditions, which are called normal:

- G=800 W/m^2,
- T_{amb}=20 ºC,
- V_{wind}=1 m/s.

Previous equation (Equation 6) can also be written as,

$$T_{cell} = T_{amb} + \frac{G}{h} \quad (7)$$

Where:

- T_{cell}: Temperature of the PV cells of the plant [ºC],
- T_{amb}: Ambient temperature measured by the ambient temperature sensor [ºC],
- G: Solar irradiance [W/m^2],
- h: convection parameter of the PV modules [W/Km^2].

For the PV modules in the plant, NOCT = 47 ºC (or h = 29,63 W/Km^2), whereas ambient temperature and solar irradiance are specific to each measurement time.

As it was done with the case of the solar irradiance, it is worthy explaining how the cell temperature measurement would be made with the reference solar cell. With the specifications from Table 8, it is known the voltage signal for a cell temperature of 25 ºC and the rate of variation of that voltage signal. See Equation 8.

$$T_{cell} = \frac{V_{OC} - V_{OC}(T_{STC})}{\beta} + T_{STC} = \frac{586{,}7 - V_{OC}}{2{,}17} + 25 \quad (8)$$

Where T_{STC} is the cell temperature under standard test conditions (25 ºC).

After calculating the cell temperature, it is possible to calculate the *k(T)* correction for Equation 3. See Equation 9.

$$k(T) = \frac{1}{1 + \frac{T_{cell} - 25}{100} \cdot k_{VMPP}} \quad (9)$$

Therefore, the final equation for the corrected power is Equation 10:

$$P_{corr} = P \cdot \frac{1}{1 + \frac{T_{cell} - 25}{100} \cdot k_{VMPP}} \quad (10)$$

3.3.3. Power output and ambient conditions

Once information about the performance of the PV plant is linked with minutely ambient conditions, a relation between them can be set. The sought relation links the corrected power output (estimation for T_{cell}=25 ºC) and solar irradiance for the PV modules. Since solar irradiance and output power are directly related, it is easy to estimate the power output for different irradiances once the relation is set.

It is important to have the corrected output power because the power is very dependent on ambient conditions, including temperature. Therefore, if trying to find a linear relation between irradiance and output power (as it is supposed to be, explained in EFECT OF IRRADIANCE AND TEMPERATURE) without the corrected power, the relation would not be linear, because cell temperature increases as irradiance and output power do.

To find the relation between irradiance and output power, Microsoft Excel is used again. With multiple data points of power and irradiance it is possible to perform a regression analysis via least squares method. As it has been mentioned multiple times, the relationship that is expected from those variables is a linear one, therefore the equation of a straight line is obtained, with the following form.

$$P_{T=25\,ºC} = m \cdot G + x_0 \quad (11)$$

Adjusting *m* and x_0 parameters will allow estimating the new nominal power of the panels.

3.3.3.1. New STC power

Basing the calculation of the new power under STC on the relation between output power and solar irradiance, it is easy to estimate the new nominal power of the plant. The calculation will be an extrapolation of the measurements made for 4 strings of PV modules.

Taking the linear relation found for power output, solar irradiance is going to be substituted with 1000 W/m^2, the irradiance level for STC. See Equation 12.

$$P_{STC}^{new}(W) = m \cdot 1000 + x_0 (\frac{W}{m^2}) \quad (12)$$

This new nominal power will be the one compared to the original nominal power of the plant, which is in the datasheet of the plant: 63,7 kWp.

3.3.3.2. k_{MPP} estimation

Since the correction of the power is done based on the thermal coefficients of the PV modules, it is important to guarantee that these parameters are consistent with reality. For that purpose, the k_{VMPP} parameter will be estimated basing on the measurements done in the inverter 2.1.

The estimation of the parameter will be done considering that k_{MPP} and k_{VMPP} are very similar parameters. Therefore, k_{VMPP} will be calculated for each timestep of the minutely data using the equation 13.

$$k_{MPP} = k_{VMPP} = \frac{100}{T_{cell} - 25} \cdot (\frac{V_{MPP}^{meas}}{V_{MPP}^{STC}} - 1) \quad (13)$$

3.3.3.3. *Cell temperature calculation*

However, even if k_{MPP} coefficient influences Equation 8, cell temperature should also be considered when regarding to the accuracy of the results. Equation 6 shows how cell temperature is calculated based on ambient temperature. Here, the NOCT parameter from the datasheet of the PV modules is used. In this case, the NOCT of 47 ºC is equivalent to having a convection parameter of 29,63 W/Km^2. This is, nevertheless, a too high value according to previous research carried out in the university (Júlia Solanes Bosch, 2017), where it was found out that h values closer to 25 W/Km^2 are more real. Therefore, this is also going to be studied.

3.3.4. Inverter evaluation

The inverter performance evaluation will be done just in one inverter. Even if 4 strings are being monitored, just one inverter output is being measured. Therefore, the efficiency of the inverter can be easily calculated as shown in the Equation 14,

$$\eta_{inv} = \frac{P_{AC}}{P_{DC}} \tag{14}$$

Inverters usually have different rated efficiencies depending on the power they are managing. For example, *euroefficiency* considers different operating points between 5% and 100% of the nominal power of the inverter to be calculated (*Types of Inverter Efficiency Peak CEC and Euro - Solar Choice*, no date). See equation 15.

$$\eta_{EU} = 0{,}03 \cdot \eta_{5\%} + 0{,}06 \cdot \eta_{10\%} + 0{,}13 \cdot \eta_{20\%} + 0{,}1 \cdot \eta_{30\%} + 0{,}48 \cdot \eta_{50\%} + 0{,}2 \cdot \eta_{100\%} \tag{15}$$

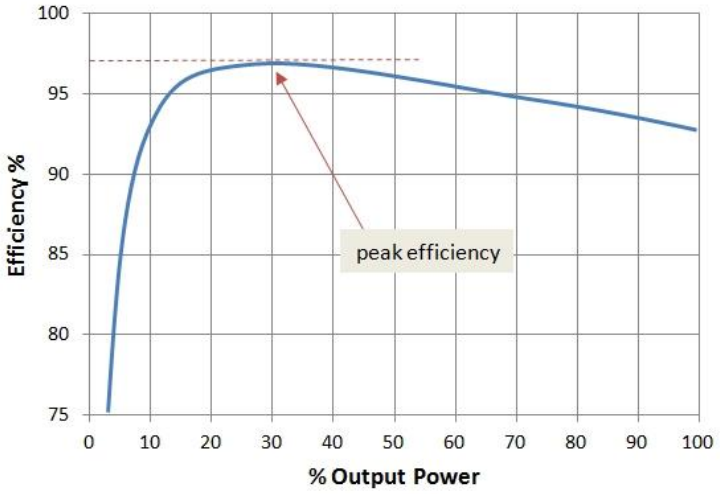

Figure 23: Efficiency of an inverter depending on work load (6.5. Efficiency of Inverters | EME 812: Utility Solar Power and Concentration, no date)

Thus, with Microsoft Excel, it is possible to calculate the *euroefficiency* of the monitored inverter and then compare it with the information of the datasheet. The same can be done with maximum efficiency, but instead of having to calculate it the maximum value is taken directly.

Information in Table 6 says that inverter original *euroefficiency* was of 95,4%, while maximum efficiency was 96,2%.

4. RESULTS

In this chapter the outcomes for the different measurements are presented. Due to environmental condition dependency for the proper analysis of the plant, a sunny day gives more information about the performance of the plant. In a sunny day, a higher irradiance diversity is had in the plant. Higher irradiance around solar noon and lower irradiance closer to the sunset. Bearing this in mind, the 5th of May is considered as the best day to study the performance of the plant.

In addition, some problems were had with the loggers in the following days. Since there is more than just one logger, all of them must be synchronised to provide useful data. Otherwise, the collected data will have different timelines, what makes very inconvenient and difficult to work with, while it is unnecessary, if proper data has been stored.

This is exactly what happened to the loggers sometime during the morning of the 6th of May. Therefore, data from the 5th of May is both useful and ready to be used, and that is why the results are based on these measurements. However, data from other days is also provided in the appendix.

4.1. IRRADIANCE AND POWER MEASUREMENTS

The solar irradiance measurement for the 5th of May are shown in Figure 24 plotted versus the hour of the day in local time (CET), not solar time. Notice how with the lack of clouds, the irradiance keeps falling until the sun hides behind the horizon (around 17:40). Since the power plant is behind a hill, this happens before sunset. After 17:40, diffuse radiation still reaches the PV modules and they receive around 60 W/m^2, which slowly decreases until sunset, at 20:45.

It is worth mentioning that a failure in the irradiance measurement device (reference solar cell) can be detected in the chart. There is a plot at the beginning of the measurement that is not in the curve formed by the rest of the measurements neither in the power outcome represented in Figure 25. Thus, the most logical thing is to assume a punctual malfunctioning of the device.

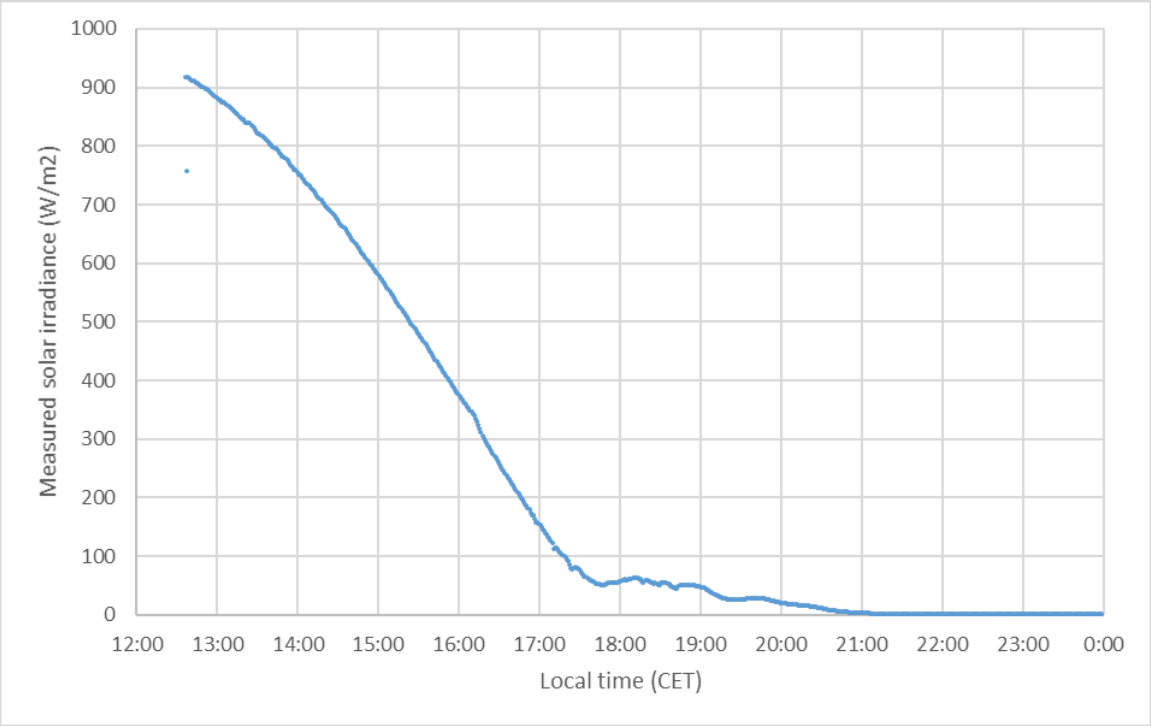

Figure 24: Measured solar irradiance, 5th of May.

Figure 25 shows the measurements for the outputs in 4 strings. Strings 1 and 3 are formed by 20 modules, whilst strings 2 and 4 are formed by 19 modules each, what leads to a 5% higher

production in odd strings. However, string 1 has around 1,3% higher production than strings3 and string 2 has over 0,6% higher production than string 4.

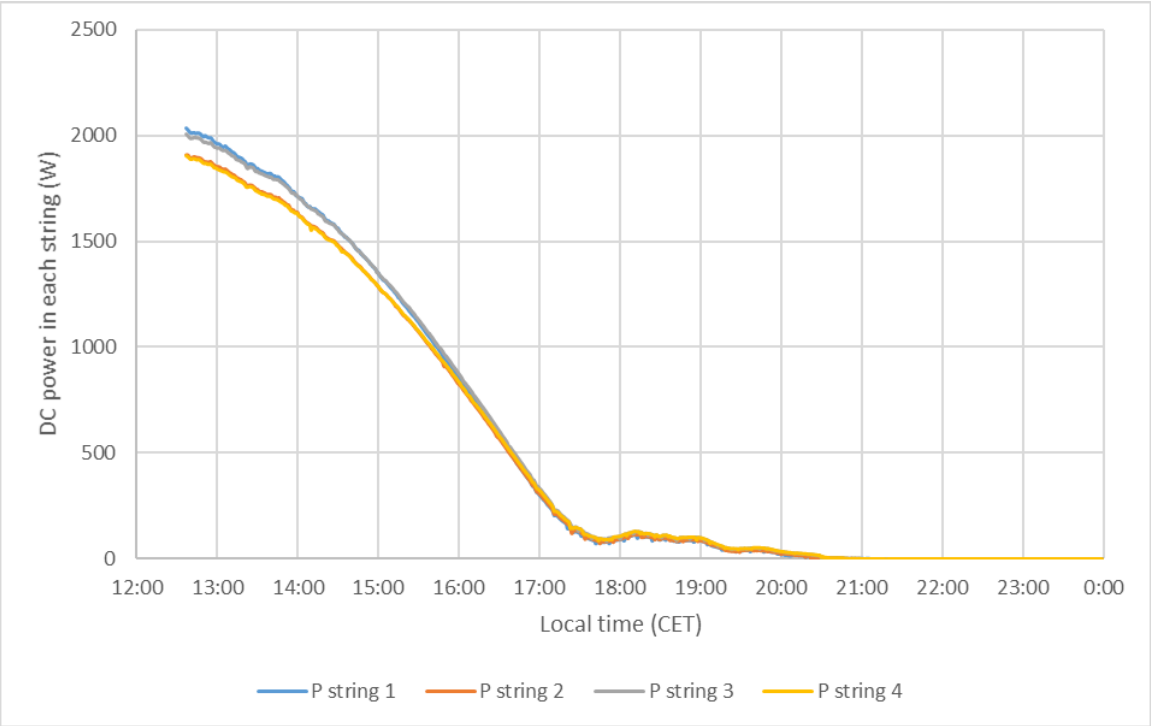

Figure 25: Measured DC power in all 4 monitored strings, 5th of May.

The power outcome seems to follow perfectly, but scaled, the irradiance measurements shown in Figure 24. This means that, as it is well known, the output power of the plant is proportional to the irradiance PV modules receive.

To have a broader view of the measurements, Figure 26 shows the measurements of both DC power outcome for the first string and irradiance measurements. During the morning and until 14:00 the irradiance evolves following a smooth curve. This happens because the angle of incidence of the sunlight changes slowly over the day. However, after 14:00, some clouds appeared causing sudden irradiation and, therefore, power drops.

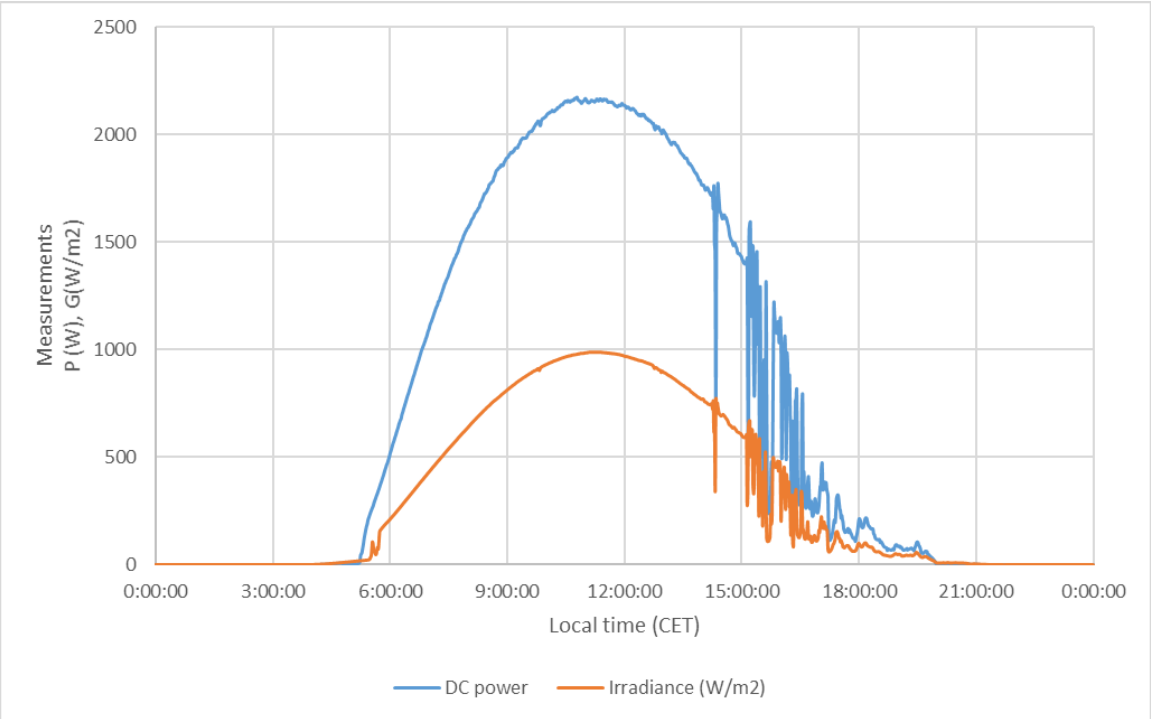

Figure 26: Solar irradiance and measured DC power in string 1, 9th of May.

4.2. PV STRING PERFORMANCE

The analysis of the results is done for all 4 measured strings. The following figures show the comparison between the measured power and the corrected power. Due to higher cell temperatures corrected power is slightly higher than measured power.

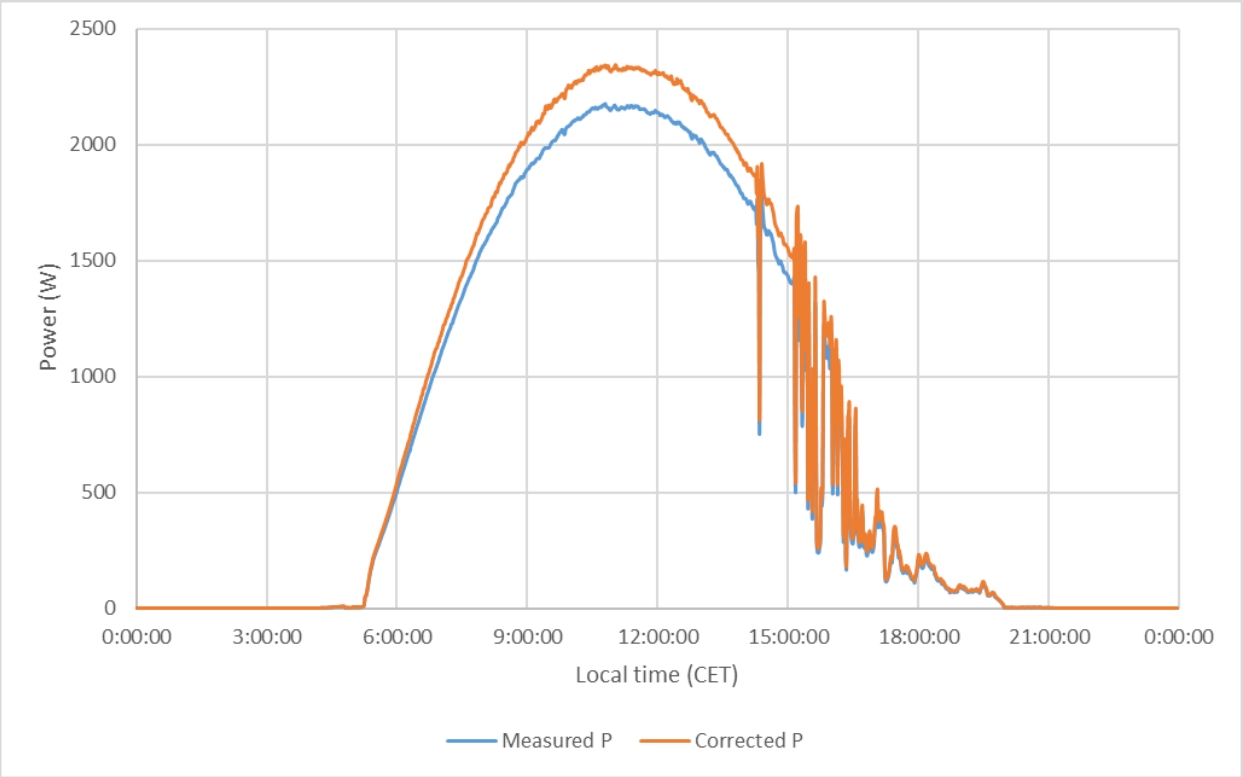

Figure 27: Measured power and corrected power vs time. 9th of May.

Figure 28 shows the measured power from string 1 and the theoretical power calculated for the string 1 basing on the irradiance and ambient temperature measurements. The assumed new nominal power of the string for this calculation is 2420 W. It can be seen how the curve adjusts quite well with this new nominal power. It is worth reminding that the original rated peak power was of 2600 W.

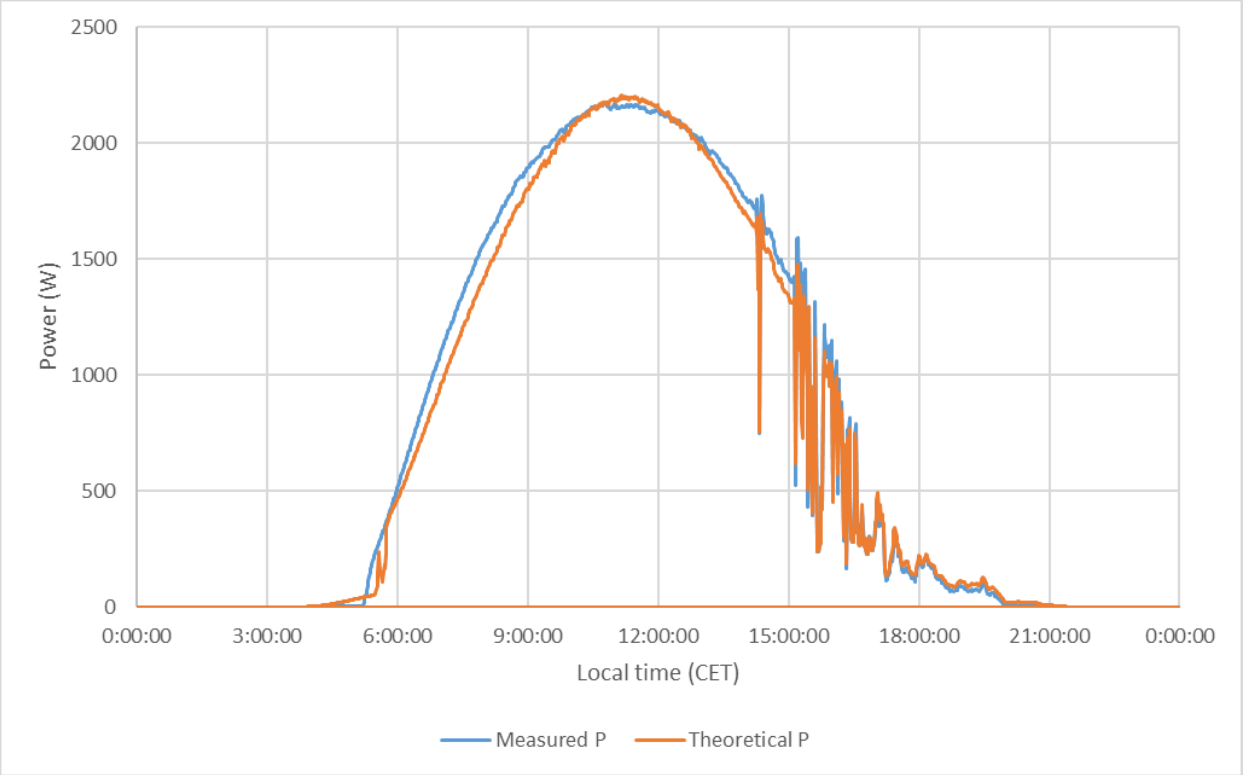

Figure 28: Measured time and theoretical power vs time. 9th of May.

Next figures represent the corrected output power plotted versus the solar irradiance, measured with the reference solar cell. Raw data in which this is based on is shown in the appendix.

Orange points are the minutely average corrected output power, while the stripped blue line is the linear approximation with the least squares method. The straight line is extended until 1000 W/m^2 to show visually the expected STC power. The equation of the straight line and the R^2 factor are also shown in the chart. See Figure 29, Figure 30, Figure 31 and Figure 32.

It can be seen how the R^2 factor is very close to 1. This means that the approximation of the relationship between solar irradiance and output power is good. However, measurements of other days show some scattering in the chart. Those charts are shown in the appendix.

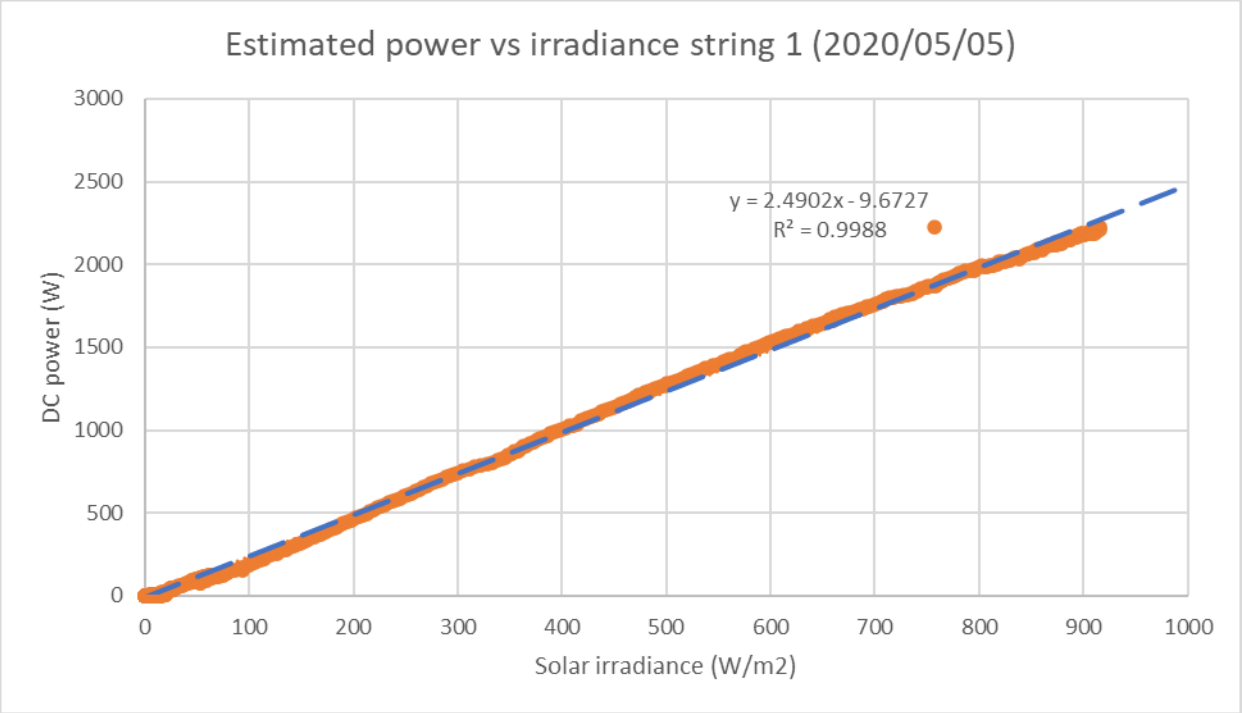

Figure 29: Corrected power output vs irradiance string 1. Estimation of the power dependant on the solar irradiance to find new STC power.

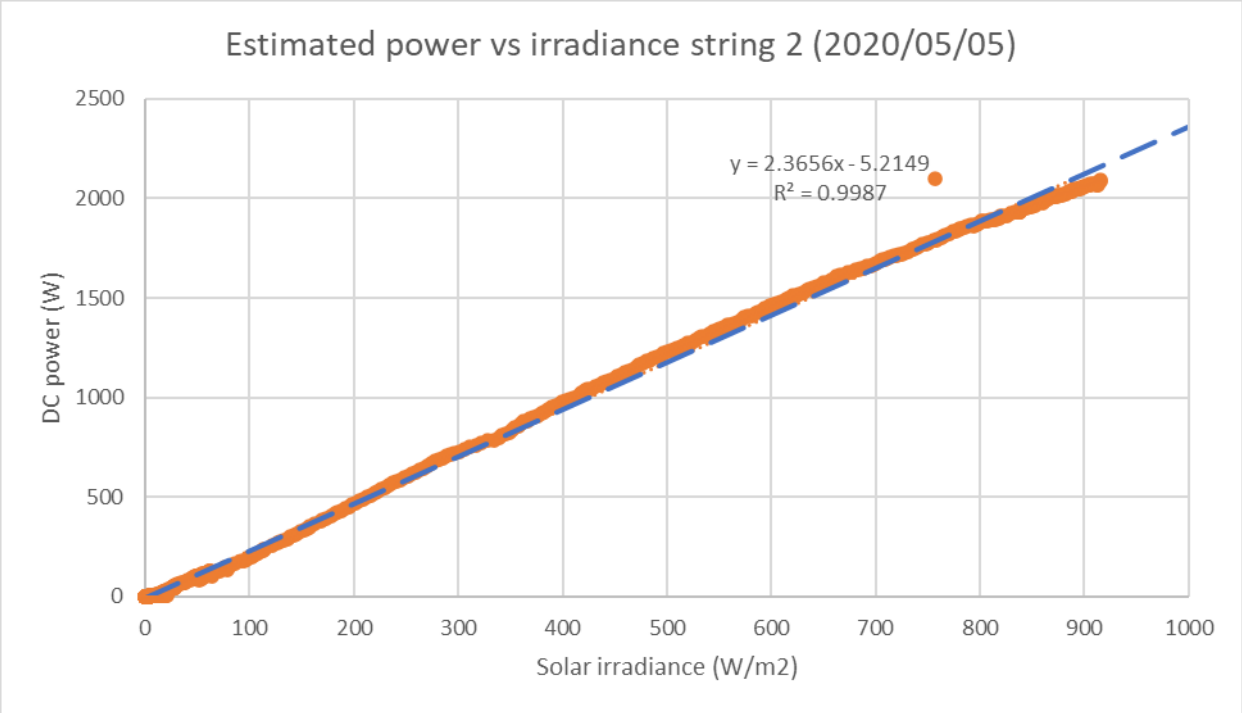

Figure 30: Corrected power output vs irradiance string 2. Estimation of the power dependant on the solar irradiance to find new STC power.

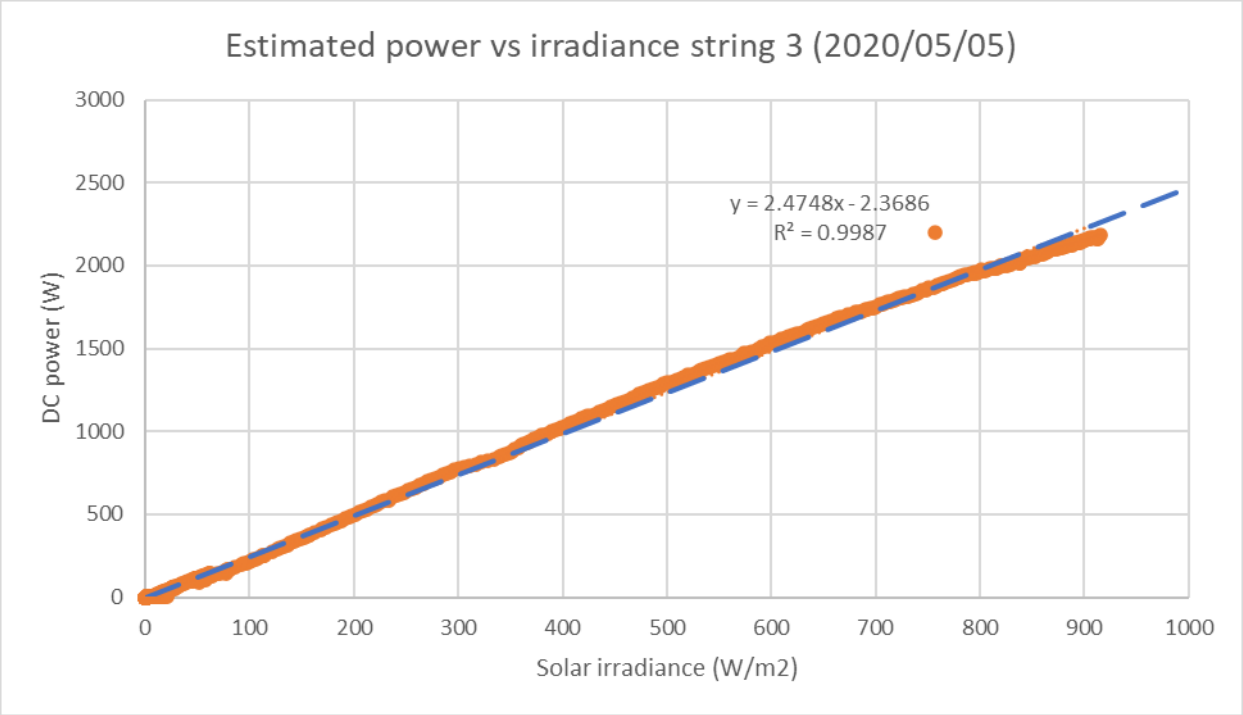

Figure 31: Corrected power output vs irradiance string 3. Estimation of the power dependant on the solar irradiance to find new STC power.

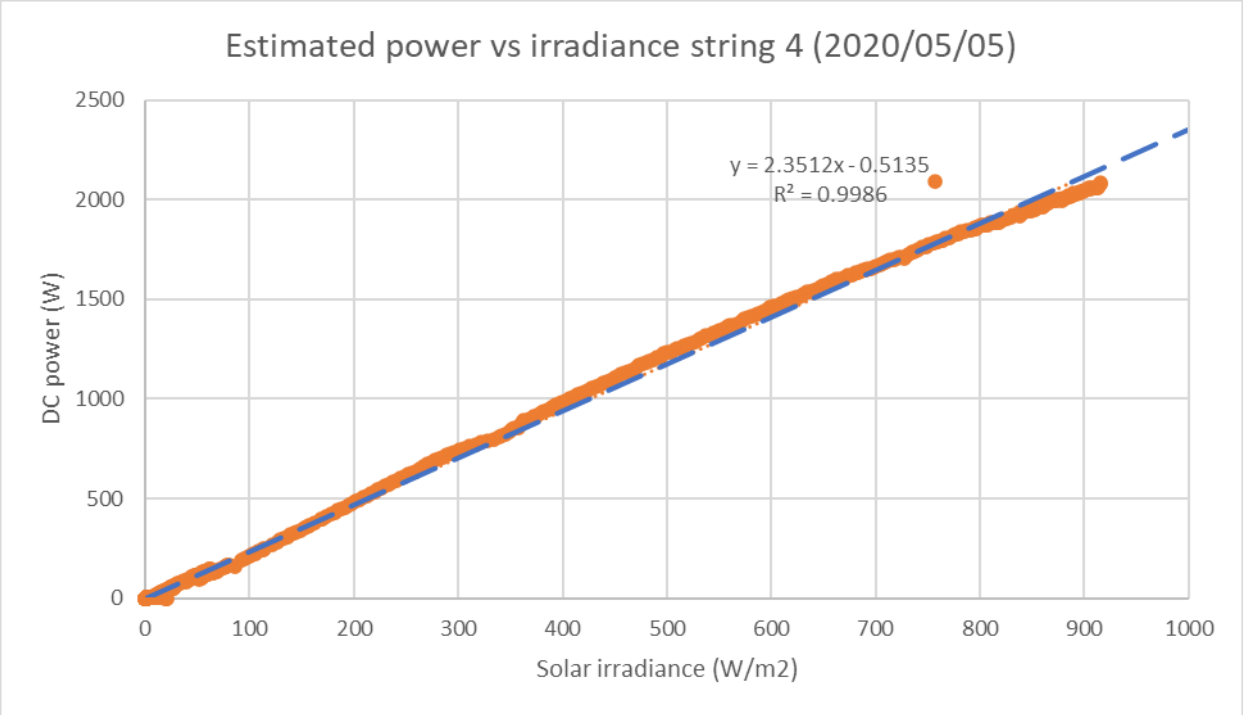

Figure 32: Corrected power output vs irradiance string 4. Estimation of the power dependant on the solar irradiance to find new STC power.

Table 9 shows the estimated power output with STC for each one of the four monitored strings. It also compares the output value with the original STC power at the moment of the installation. It shows a degradation of the PV modules of below 5% in all 4 strings.

Table 9: Estimated STC power for each string (k_{MPP} = -0,4%/ºC and h = 29,63W/Km^2).

	Number of modules	Original STC power (kWp)	Estimated STC power (kWp)	Power loss (%)
String 1	20	2600	2481	**4.60%**
String 2	19	2470	2360	**4.44%**
String 3	20	2600	2472	**4.91%**
String 4	19	2470	2351	**4.83%**

Power loss due to degradation is quite consistent for all 4 strings, they are gathered in a range of less than 0,5% of power loss. However, the loss is not very significant considering all the assumptions that have been made. For example, temperature coefficients of PV modules have been assumed in Table 4. To study the effect of the coefficients on the result the analysis is going to be repeated with different coefficients. See Table 10.

Table 10: New assumed temperature coefficients of the PV modules.

Parameter	Value
Coefficient of short circuit current	0,05%/ºC
Coefficient of open circuit voltage	-0,36%/ºC
Coefficient of maximum power	-0,35%/ºC
Coefficient of maximum power voltage	-0,35%/ºC

Table 11: Estimated STC power for each string with the new temperature coefficients (k_{MPP} = -0,35 %/ºC and h = 29,63 W/Km^2).

	Number of modules	Original STC power (kWp)	Estimated STC power (kWp)	Power loss (%)
String 1	20	2600	2452	**5.70%**
String 2	19	2470	2333	**5.55%**
String 3	20	2600	2444	**6.01%**
String 4	19	2470	2323	**5.93%**

Table 11 shows the results for the temperature coefficients assumed in Table 10. It can be noticed that power loss is now around 1,1% higher for each string. Bearing in mind that the coefficient of maximum power (k_{MPP}) is the one with more effect in the power output, its typical extreme values have been considered. Previous work (Júlia Solanes Bosch, 2017)(Compadre Senar, 2018)(Urrutia, 2017) said typical values for k_{MPP} are between -0,4%/ºC (first assumption Table 4) and -0,35%/ºC (second assumption Table 10).

Either way, with the most optimistic or pessimistic scenarios (analysed respectively) the power loss is consistent for all strings and it can be set between 4,5% and 6%. Calculating the weighted average of power loss regarding to the peak power of each string, it is found that the value of power loss is -5,25%.

4.2.1. k_{MPP} estimation results

Figure 33 shows the calculations of the k_{MPP} based on the first 100 measurements of the logger, which happen to be very representative of the PV system since the ambient conditions are quite good. The average irradiance is 826 W/m^2, with values between 915 W/m^2 and 714 W/m^2. Temperature has been recorded between 14,1 ºC and 16,7 ºC, with an average value of 15,4 ºC. According to historical data (*Clima Gävle - meteoblue*, no date), the average temperature between May and September, the months with around 74% of the yearly electricity production regarding to 2008 and 2009 daily data (see appendix), is 14,8 ºC.

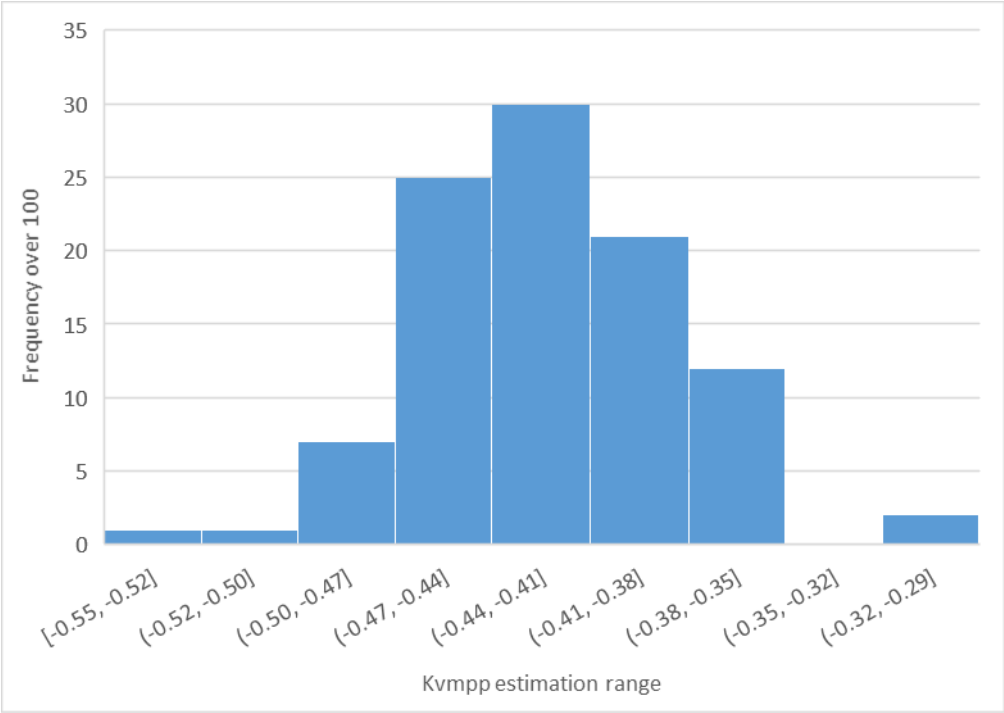

Figure 33: k_{MPP} estimation histogram based on 100 measurement timesteps.

As mentioned above, Figure 33 gives information about the estimated k_{MPP} value for the studied PV system. It can be seen how the estimated values gather mostly between values slightly higher than -0,4%/ºC. In fact, 64% of the calculations give values of k_{MPP} higher (in absolute value) than -0,41%/ºC and 75% of them values over -0,38%/ºC.

In previous subsections it has been mentioned that k_{MPP} can define an optimistic or pessimistic situation. In this case, it has been proven that the estimations and assumptions made for k_{PMPP} are less optimistic than reality, which covers the back on other inaccuracies of this study.

4.2.2. Cell temperature

Cell temperature has been calculated so that the results obtained from information in the datasheet of the PV modules can be compared to the ones obtained from previous research made in HiG. In this case, the used NOCT was of 52 ºC instead of 47 ºC. New power estimation can be seen in Table 12.

Table 12: Estimated STC power for each string with new cell temperature calculation (k_{MPP} = -0,4%/ºC and h = 25 W/Km^2).

	Number of modules	Original STC power (kWp)	Estimated STC power (kWp)	Power loss (%)
String 1	20	2600	2544	**2.14%**
String 2	19	2470	2421	**1.98%**
String 3	20	2600	2536	**2.46%**
String 4	19	2470	2411	**2.39%**

4.3. INVERTER

This subsection shows the results for the inverter efficiency measurements. Some of the same problems explained in previous sections were had when analysing data from the inverters. Since 2 different loggers were used (Fluke for the AC output of the inverter and Agilent for the DC input or the inverter) data might be slightly shifted in time. This leads to a lot of scattering when

plotting the results and makes very difficult to work with the collected information. Thus, to be able to use the data, it has been sorted in different groups.

Figure 34 shows the data of the first 500 measurements. As it can be seen, the chart shows a quite smooth line. The average efficiency of the inverter in this data group is 94,3%.

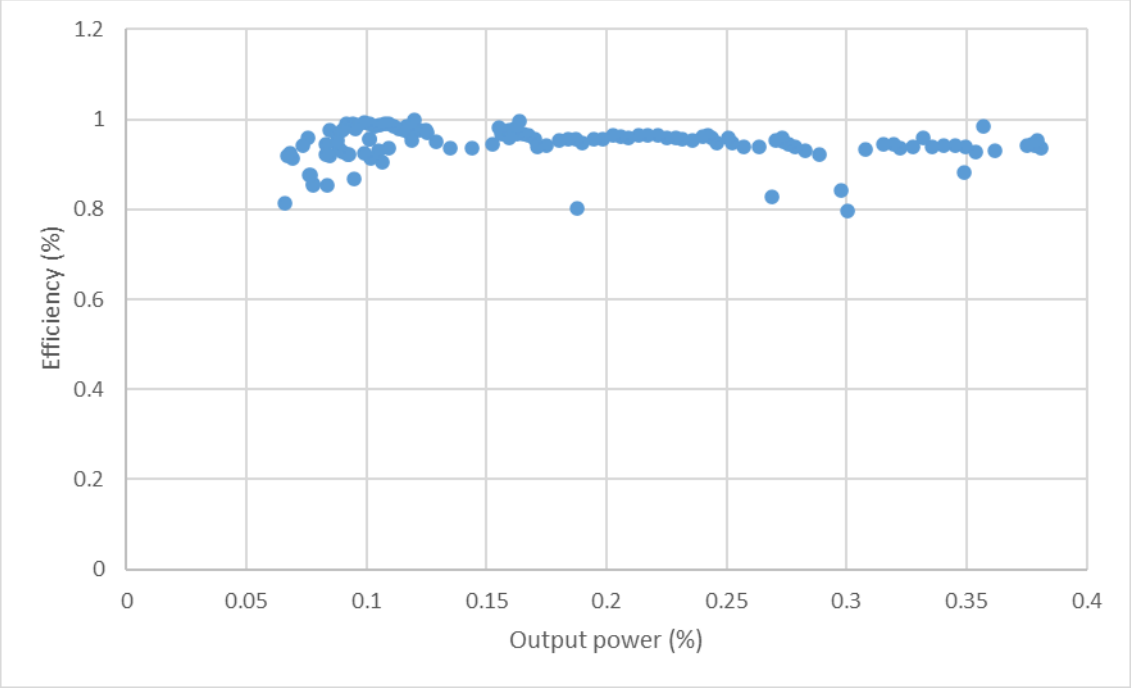

Figure 34: Graphical representation of inverter efficiency vs workload (500 points).

Figure 35 shows the data of the first 1000 measurements. As it can be seen, the chart shows more scattering than the chart of the first 500 measurements. The average efficiency of the inverter in this data group is 93,2%.

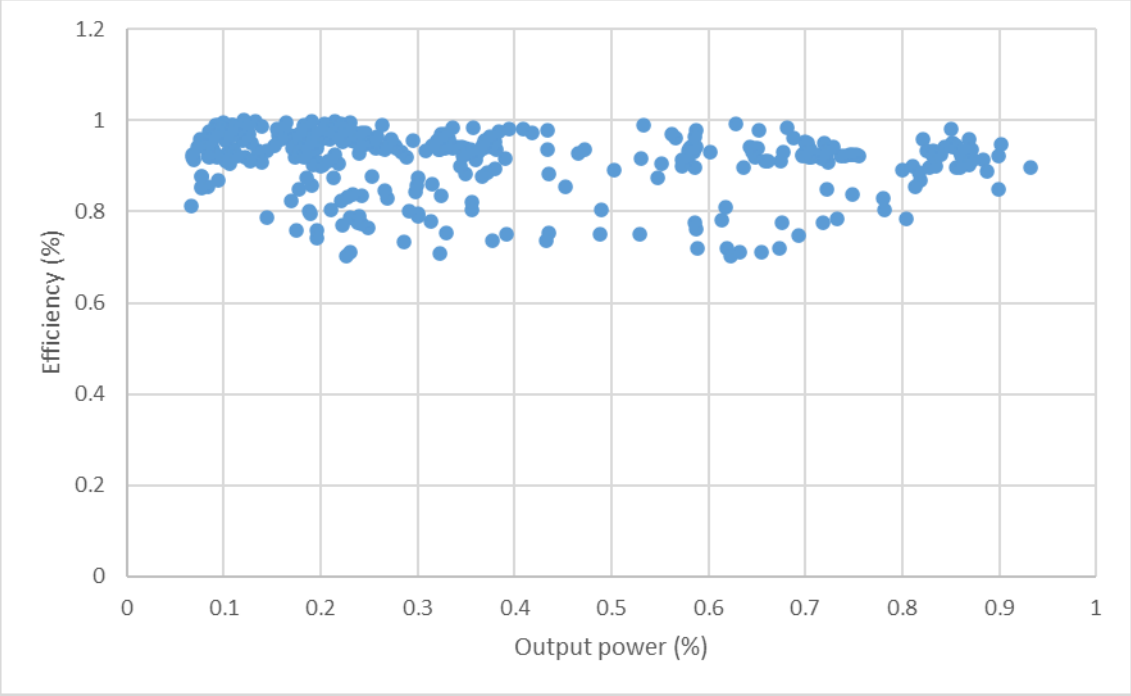

Figure 35: Graphical representation of inverter efficiency vs workload (1000 points).

Figure 36 shows all the data of the. As it can be seen, now the scattering is quite large. Not sorting the data makes more difficult to take useful information from it. The average efficiency of the inverter in this data group is 92,8%. It is worth mentioning that the scattering is reduced as the output power increases.

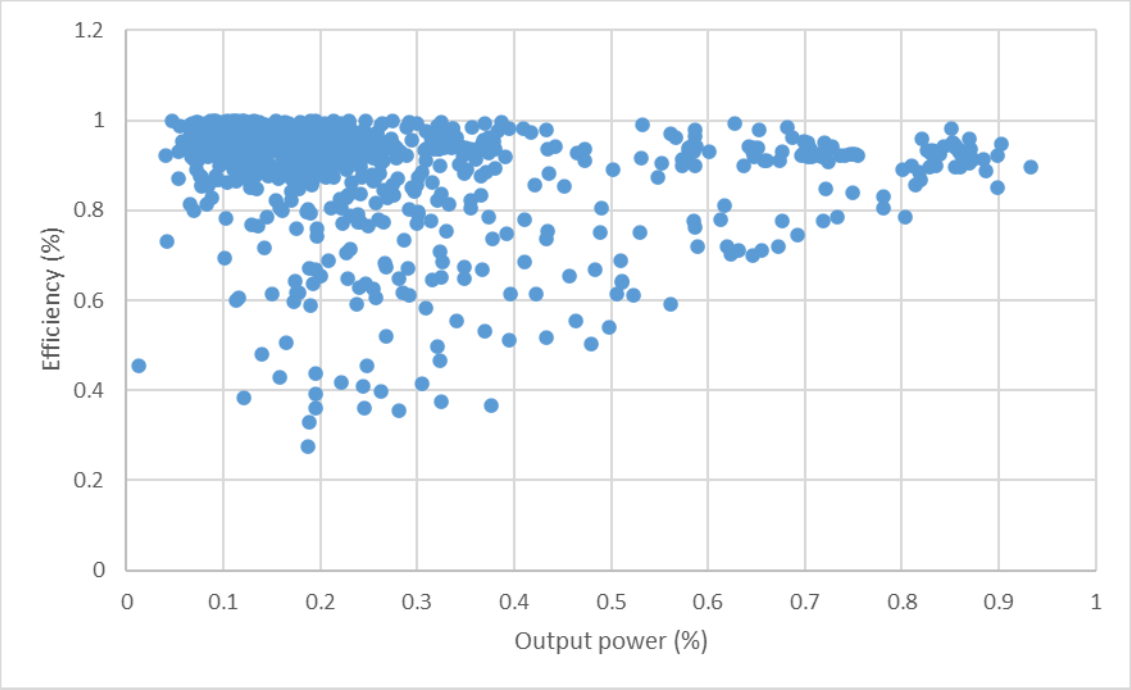

Figure 36: Graphical representation of inverter efficiency vs workload (all points).

5. DISCUSSION

First of all, it is important to define the aim of the study and how the results will be analysed to achieve that aim. The goal of the paper is to determine how the PV plant has aged and how has it degraded with time. For that purpose, the main tool has been the monitoring of four of the DC strings, located in the Part B of the plant, in the roof of the church. In addition, current and voltage measurements were also made in the output of one of the inverters. The first measurements will serve to evaluate the performance of the PV modules but also of the MPPT algorithm of the inverters. On the other hand, the second set of data will only be used to analyse the inverter performance. The degradation will be estimated as a power loss, but there are no mechanisms to analyse the cause of this degradation. However, in THEORETICAL BACKGROUND some aging mechanisms have been analysed and explained.

5.1. RELIABILITY OF THE MEASUREMENTS

As it has been explained in previous chapters, there have been some problems with the different dataloggers. Those problems have been related to the specific timeline of each of the dataloggers, meaning that when whilst all of them record the data for a specific time, the recorded time might not be the same for different loggers.

This problem was had after the first day of measurements, 5th of May. The time shifting was estimated to be of 5 seconds between the two Agilent loggers, responsible for the irradiance and temperature measurements and for the DC power output.

However, having this kind of problems does not mean the measurements are wrong, because the sensors may still work properly. This leads to more difficult data analysis after the first day, therefore, all the calculations were done with the data from the 5th of May.

Using data from just one day might be not very representative of the PV plant's performance, yet, being a sunny day and having recorded minutely data gives a lot of measurements to have a more reliable basis to work with.

On the other hand, the reliability of the sensors can be also discussed. Figure 26 shows some problems with the irradiance measurements before 6 a.m. The DC power increases smoothly due to the sunrise and greater irradiance; however, the first irradiance measurements do not seem to follow the same smooth trend, probably to some problems in the measurements. However, the rated accuracy of the power and irradiance is in the order of 5%, so there should not be any problem with measurements.

5.2. PV MODULE AGING

It is worth bearing in mind that the study was performed in the Part B of the PV plant, where the PV modules are located directly on the roof of the building. In Part A, the modules are located in some stands that lie on the roof of another building. These stands are more likely to cause mismatch losses in the strings because they might not be properly aligned.

Figure 37 shows the unalignment of the PV strings in the Part A of the plant due to not properly placing the stands. This problem is not had in the Part B, where the PV modules lie on the surface of the roof.

Therefore, if the measurements would have been taken on the Part A of the plant, it is more likely that the power reduction had been higher. However, this power drop would not be real, and it would be due to mismatch losses, which are quite difficult to calculate. Thus, not having this problem in Part B of the plant make the obtained results more reliable.

Figure 37: PV arrays not properly aligned in Part A of the plant. This causes mismatch losses.

The conclusions that can be drawn from the DC power measurements when related to solar irradiance are that the performance of the plant does not seem to have suffered a big degradation. Depending on the estimated k_{MPP} coefficient, power loss is between 6% and 4,5%. These power loss rates do not represent a disturbing degradation for a 13-year-old PV power plant.

In addition, it has been mentioned before the dependency of the power loss estimations with the k_{MPP} coefficient. Therefore, and since the k_{MPP} coefficient has also been approximately guessed basing on different papers, an estimation of it was also made in this paper.

While when assumed, the k_{MPP} coefficient was studied to be between -0,35%/ºC and -0,4%/ºC, the estimations showed that it would be slightly higher, around -0,425%/ºC. It is important to bear in mind that lower k_{MPP} coefficients (in absolute value) mean greater power loss of the PV modules, whilst higher k_{MPP} coefficients (in absolute value) mean smaller degradation of the PV modules. Therefore, if the real estimated k_{MPP} coefficient is actually slightly higher (in absolute value) than the assumed value, this would mean that the real degradation of the PV modules would be lower than 4,5%.

Since NOCT also affect the calculations of theoretical STC power (see Equation 10 and Equation 6), its effect in the power loss calculations have been considered too. Table 12 shows that the average power loss in all 4 strings is reduced from around 4,5% to less than 2,25% when considering a NOCT of 52 ºC, as previous work did. Therefore, the real power loss might be even smaller than mentioned above if the cell temperature is higher than calculated, i.e. if the real NOCT is closer to 52 ºC than to 47 ºC.

Considering that PV module manufacturers provide a 25 year long 80% production warranty, the degradation during the first half of that time meets the warranty of the manufacturers.

Regarding to the specific results of each one of the monitored arrays there is a fact that is worth mentioning. String 1 and 3 have 20 PV modules each, while string 2 and 4 have 19 each. Therefore, the expected power production should be the same for odd strings and for even strings. However, as Figure 25 shows, strings 3 and 4 have slightly less power output than strings 1 and 2. This might be due to mismatch losses if string 3 and 4's PV modules have been placed incorrectly. This may as well be owing to manufacturing difference, since the output difference

is of just around 1,3% for odd strings and of approximately 0,6 for even strings and the nominal power of the PV modules at the production time had an accuracy of 3,85%.

This causes are, nevertheless, quite a coincidence since both strings with lower production are connected to the same inverter (2.2). Hence, the cause of the power difference could come from the inverter itself. The responsible for extracting the maximum power from the PV strings is the MPPT algorithm. If the MPPT algorithm is not updated or does not work properly, it could be the reason for the power output difference. However, the straight lines in Figure 29, Figure 30, Figure 31 and Figure 32 are an indication that the MPPT is working for all currents.

Even so, just information from 2 inverters is not enough to determine the causes of the power difference. It might come from differences in the inverters, but it is true that one would expect those differences to be the same for both strings, while they are almost double for strings 1 and 3. Therefore, coincidental causes are assumed as the responsible for this fact.

Regarding to the reasons for this degradation, the main factors were already explained in LITERATURE REVIEW. First of all, PID has a grater effect in bigger PV plants, where having the first module of each array connected to earth causes too big earth currents, and where PV arrays have a voltage of up to 1500 V. For this plant, the greatest voltage through the array that can be kept in time would be the V_{MPP}, where the PV modules are working with a low cell temperature (25 ºC). Table 3 shows that this voltage is of 16,9 V, therefore, for the strings with more PV modules, 20 modules, the maximum voltage would be 338 V. Even considering the open circuit voltage the array voltage would be 440 V.

This means that in the worst case, the maximum reverse voltage between the frame of the modules and the PV cells themselves would be of 440. However, for this to happen the last PV module's positive terminal would have to be connected to earth. This makes no sense, and therefore, if the array is not connected to ground potential and the middle point takes earth potential, then the maximum reverse voltage would be 220 V.

This level of voltage does not cause a noticeable effect due to PID, what may explain why the modules have degraded so little.

Aside from this, EVA encapsulation of modules can degrade with time and, if it is rough, with climate effects too. As mentioned before, cold weathers like the one of Gävle help this kind of degradation from happening. Therefore, this gives another reason for such a small power loss in the plant.

5.3. INVERTER AGING

Regarding to the inverter performance, it is difficult to evaluate its degradation due to a great scattering in almost all the measurements. Despite this, the obtained results show that the efficiency of the inverter is way above 90%. While the rated *euroefficiency* of the inverter is 95,4% as shown in Table 6, the measured average efficiency was of between 92,8% and 94,3%. This accounts for a degradation of between 1,15% and 2,73% referring to the power conversion from DC to AC.

That degradation rate is very small, but it is worth bearing in mind that degradation in power electronics usually leads to completely shutting down devices, instead of progressively reducing their efficiency, as it happens with PV modules. Thus, it is most likely that this degradation is due to corrosion or physical degradation in the terminals or in the contact points.

Regarding to a fact mentioned before, given that, theoretically, strings 1 and 3 and 2 and 4 have to be the same since they have the same number of modules, if their production difference (1,3% and 0,6% respectively) comes from the inverter this would mean that there exist a power loss not

related to power conversion from DC to AC. Instead, this could be caused by a difference in the MPPT algorithm in the inverters. Maybe due to different types of algorithms or due to updates in the software that were not applied to all inverters.

However, this is something that cannot be determined just with the measurements that were took. Thus, those ideas are left as hypothesis to what could cause the current behaviour of the PV plant.

5.4. PV PLANT OVERALL AGING

Considering all the factors that might have an effect in the performance of the PV plant as a whole system, ,i.e. PV modules and power inverters mainly, it has to be said that the total measured efficiency of the plant has been of 88,8%. For this calculation, a degradation of 4,5% was taken in the PV modules and an efficiency of 93% in the inverters. Bearing in mind that modern inverters usually have an efficiency of at least 98%, substituting the inverter with a modern one can lead to an increased efficiency of 93,6%, meaning that the power loss due to degradation would be almost completely mitigated.

Regarding to the power loss due to degradation, approximately a 2% power loss is caused owing to inverter degradation, while the same 4,5% is due to PV module aging. Therefore, a total power loss of 6,4% is estimated after the measurements.

However, there is a factor that is let unmentioned due to the difficulty to measure it. Mismatch losses are a very important fact that leads to power reduction. Even if in Part B of the plant there are no mismatch losses, in Part A (the biggest part of the plant) the PV modules are not perfectly aligned in each string. Even though mismatch losses are not very high in the middle of the day, when the irradiance is higher, they have bigger effect when the sun is closer to the horizon.

A proper construction of the PV plant is something that may take more time when building it, but will increase the generated power is the mismatch losses are reduced. Therefore, it can be said, as an indication, that better safe than sorry.

6. CONCLUSIONS

After the performed analysis of the obtained data it is interesting to extract some conclusions about the work.

Firstly, regarding to the measurement reliability and the logging devices, it is obvious that some improvements could have been made. The problems that were had with the loggers could have been solved using a single data logger to record and collect all the data from DC power, AC power and ambient conditions. This, however, would have required communication between the sensors on the roof and the loggers in the inverter room. This is usually done using a short cable, like an USB, which can be as long as 5 meters. For longer distances, wireless transmission is often used, but this can present problems too, so there is no easy solution due to the distance from the inverters to the roof.

Regarding to the sensors, even if the reference solar cell has a different angular sensitivity than the pyranometer, it worked properly. In addition, there was also a pyranometer, which could have been used, if needed, to compare the irradiance measurements to the measurements from the reference solar cell. However, it was not considered essential to do so. The measuring board had a photodiode installed too, so even more measurements could be available for a future research about this.

About the output power predictions, it can be said that the used model work properly when the data came from loggers without time shifting. It proved to work correctly since the R^2 values were very close to 1.

As regards to the available data for comparisons, the weak point of the study is that the nominal power was not measured directly after the installations. The obtained results after the measurements taken in 2020 should have been compared to measurements taken in 2008, however there is no data from back then except the daily electricity production, which is not very useful if it is not related to irradiance measurements. Therefore, this makes difficult to extract conclusive results when the estimated degradation has been so low.

With respect to the monitored parameters, it would have been interesting to analyse all the strings of the plant, or at least strings from both Part A and Part B of the plant. This was not done, nevertheless, since there were some problems with the connections to the junction box, so finally just 4 strings were monitored. A future research could focus on finding the differences between the performance of different parts of the plant.

The same thing happens with the inverters. Just the output power of one of them was analysed, which added to the fact that more difficulties appeared because of using different loggers, meant that it was quite difficult to extract conclusive resolutions about its performance and degradation. Solving the problem of the loggers would enable performing all these analysis in an appropiate way.

Lastly, it also important to bear in mind that this study was performed just with data taken in a day in May. It would be very interesting to monitor the system the whole year to compare the results with previous years. Because of climate change and global warming, it snows less in Gävle (and everywhere) than it used to. For example, in 2020, the snow did not cover completely the panels for more than a day, what enabled to have power generation in the winter months. As it can be seen from the data recorded in 2008 and 2009, during the winter there was no production because the modules were covered in snow.

Climate change and global warming are a real concern and renewable energies are a way to fight them back. This, nevertheless, does not mean that their effect cannot be somehow beneficial in some ways. A higher electricity production due to clear modules could be analysed. However, the

opposite effect had to be analysed too. Higher temperatures reduce PV voltage, which lead to lower output power. Figuring out whether this balance means higher or smaller production would be very interesting.

7. REFERENCES

6.5. Efficiency of Inverters | EME 812: Utility Solar Power and Concentration (no date). Available at: https://www.e-education.psu.edu/eme812/node/738 (Accessed: 10 May 2020).

Chanchangi, Y. N. *et al.* (2020) 'Dust and PV Performance in Nigeria: A review', *Renewable and Sustainable Energy Reviews*. Elsevier Ltd, p. 109704. doi: 10.1016/j.rser.2020.109704.

Chen, J. (2011) *Solar energy to the Earth - Energy Education, Physics of Solar Energy*. Available at: https://energyeducation.ca/encyclopedia/Solar_energy_to_the_Earth (Accessed: 21 April 2020).

Clima Gävle - meteoblue (no date). Available at: https://www.meteoblue.com/es/tiempo/historyclimate/climatemodelled/gävle_suecia_2712414 (Accessed: 14 May 2020).

Compadre Senar, D. (2018) 'Performance evaluation of a rooftop solar photovoltaic power plant in the Gävle Arenaby (Gävle, Sweden): Installation testing', 43(June), pp. 130–138. doi: 10.1016/j.esd.2018.01.006.

Cuce, E., Cuce, P. M. and Bali, T. (2013) 'An experimental analysis of illumination intensity and temperature dependency of photovoltaic cell parameters', *Applied Energy*. Elsevier Ltd, 111, pp. 374–382. doi: 10.1016/j.apenergy.2013.05.025.

Curve Tracing FAQ's | Seaward Group USA (no date). Available at: https://www.seaward-groupusa.com/userfiles/curve-tracing.php (Accessed: 2 May 2020).

EIA, E. I. A. (2019) 'Cost and Performance Characteristics of New Generating Technologies', *Annual Energy Outlook 2019*, 2019(January), pp. 1–3. Available at: https://www.eia.gov/outlooks/aeo/assumptions/pdf/table_8.2.pdf.

Fill Factor | PVEducation (no date). Available at: https://www.pveducation.org/pvcdrom/solar-cell-operation/fill-factor (Accessed: 2 May 2020).

González, R. *et al.* (2007) 'Transformerless inverter for single-phase photovoltaic systems', *IEEE Transactions on Power Electronics*, 22(2), pp. 693–697. doi: 10.1109/TPEL.2007.892120.

González, R. *et al.* (2008) 'Transformerless single-phase multilevel-based photovoltaic inverter', *IEEE Transactions on Industrial Electronics*, 55(7), pp. 2694–2702. doi: 10.1109/TIE.2008.924015.

Gonzalez Senosiain, R., Marroyo, L. and Barrios, E. (2014) *Instalaciones grandes plantas fotovoltaicas*.

Gubía, E. *et al.* (2007) 'Ground currents in single-phase transformerless photovoltaic systems', *Progress in Photovoltaics: Research and Applications*, 15(7), pp. 629–650. doi: 10.1002/pip.761.

Hoffmann, S. and Koehl, M. (2014) 'Effect of humidity and temperature on the potential-induced degradation', *Progress in Photovoltaics: Research and Applications*, 22(2), pp. 173–179. doi: 10.1002/pip.2238.

Influencia de la irradiación y temperatura sobre una placa fotovoltaica « Ingelibre (no date). Available at: https://ingelibreblog.wordpress.com/2014/11/09/influencia-de-la-irradiacion-y-temperatura-sobre-una-placa-fotovoltaica/ (Accessed: 2 May 2020).

IV Curve | PVEducation (no date). Available at: https://www.pveducation.org/pvcdrom/solar-cell-operation/iv-curve (Accessed: 2 May 2020).

Jordan, D. C. and Kurtz, S. R. (2013) 'Photovoltaic degradation rates - An Analytical Review',

Progress in Photovoltaics: Research and Applications, pp. 12–29. doi: 10.1002/pip.1182.

Júlia Solanes Bosch (2017) 'Investigation of the performance of a large PV system', (June). Available at: http://www.diva-portal.org/smash/get/diva2:1138526/FULLTEXT01.pdf.

Liu, Z. *et al.* (2019) 'Quantitative analysis of degradation mechanisms in 30-year-old PV modules', *Solar Energy Materials and Solar Cells*. Elsevier B.V., 200. doi: 10.1016/j.solmat.2019.110019.

López-Escalante, M. C. *et al.* (2016) 'Polyolefin as PID-resistant encapsulant material in PV modules', *Solar Energy Materials and Solar Cells*. Elsevier, 144, pp. 691–699. doi: 10.1016/j.solmat.2015.10.009.

Lundqvist, M., Helmke, C. and Ossenbrink, H. A. (1997) 'ESTI-LOG PV plant monitoring system', *Solar Energy Materials and Solar Cells*. Elsevier, 47(1–4), pp. 289–294. doi: 10.1016/S0927-0248(97)00051-2.

Mamajek, E. E. *et al.* (2015) 'IAU 2015 Resolution B3 on Recommended Nominal Conversion Constants for Selected Solar and Planetary Properties', pp. 1–6. Available at: http://arxiv.org/abs/1510.07674.

Omazic, A. *et al.* (2019) 'Relation between degradation of polymeric components in crystalline silicon PV module and climatic conditions: A literature review', *Solar Energy Materials and Solar Cells*. Elsevier B.V., 192, pp. 123–133. doi: 10.1016/j.solmat.2018.12.027.

Rodrigo, P., Gutiérrez, S. and Guerrero, L. A. (2015) 'Shading in high-concentrator photovoltaic power plants', *Green Energy and Technology*. Springer Verlag, 190, pp. 177–208. doi: 10.1007/978-3-319-15039-0_7.

Sampaio, P. G. V. and González, M. O. A. (2017) 'Photovoltaic solar energy: Conceptual framework', *Renewable and Sustainable Energy Reviews*. Elsevier Ltd, pp. 590–601. doi: 10.1016/j.rser.2017.02.081.

Sera, D. and Baghzouz, Y. (2008) 'On the impact of partial shading on PV output power', *Renewable energy sources*, pp. 229–234. Available at: https://www.researchgate.net/publication/259786752_On_the_impact_of_partial_shading_on_PV_output_power (Accessed: 5 May 2020).

Silvestre, S. and Chouder, A. (2008) 'Effects of shadowing on photovoltaic module performance', *Progress in Photovoltaics: Research and Applications*, 16(2), pp. 141–149. doi: 10.1002/pip.780.

Types of Inverter Efficiency Peak CEC and Euro - Solar Choice (no date). Available at: https://www.solarchoice.net.au/blog/types-of-solar-inverter-efficiency/ (Accessed: 10 May 2020).

Urrutia, L. Z. (2017) 'Measurements and simulations of the performance of the PV systems at the University of Gävle Measurements and simulations of the performance of the PV systems at the University of Gävle'.

Wang, F. H. *et al.* (2007) 'New current programmed pixel circuit for active-matrix organic light-emitting-diode displays', in *IEEE Conference on Electron Devices and Solid-State Circuits 2007, EDSSC 2007*, pp. 1151–1154. doi: 10.1109/EDSSC.2007.4450332.

Willson, R. C. and Mordvinov, A. V. (2003) 'Secular total solar irradiance trend during solar cycles 21-23', *Geophysical Research Letters*. American Geophysical Union (AGU), 30(5), p. n/a-n/a. doi: 10.1029/2002gl016038.

World Energy Consumption Statistics | Enerdata (no date). Available at: https://yearbook.enerdata.net/total-energy/world-consumption-statistics.html (Accessed: 2 May 2020).

Woyte, A., Nijs, J. and Belmans, R. (2003) 'Partial shadowing of photovoltaic arrays with different system configurations: Literature review and field test results', *Solar Energy*. Elsevier Ltd, 74(3), pp. 217–233. doi: 10.1016/S0038-092X(03)00155-5.

Zaoui, F. *et al.* (2015) 'A Combined Experimental and Simulation Study on the Effects of Irradiance and Temperature on Photovoltaic Modules', in *Energy Procedia*. Elsevier Ltd, pp. 373–380. doi: 10.1016/j.egypro.2015.07.393.

APPENDIX I: POWER AND IRRADIANCE MEASUREMENTS

A. DAILY RAW DATA

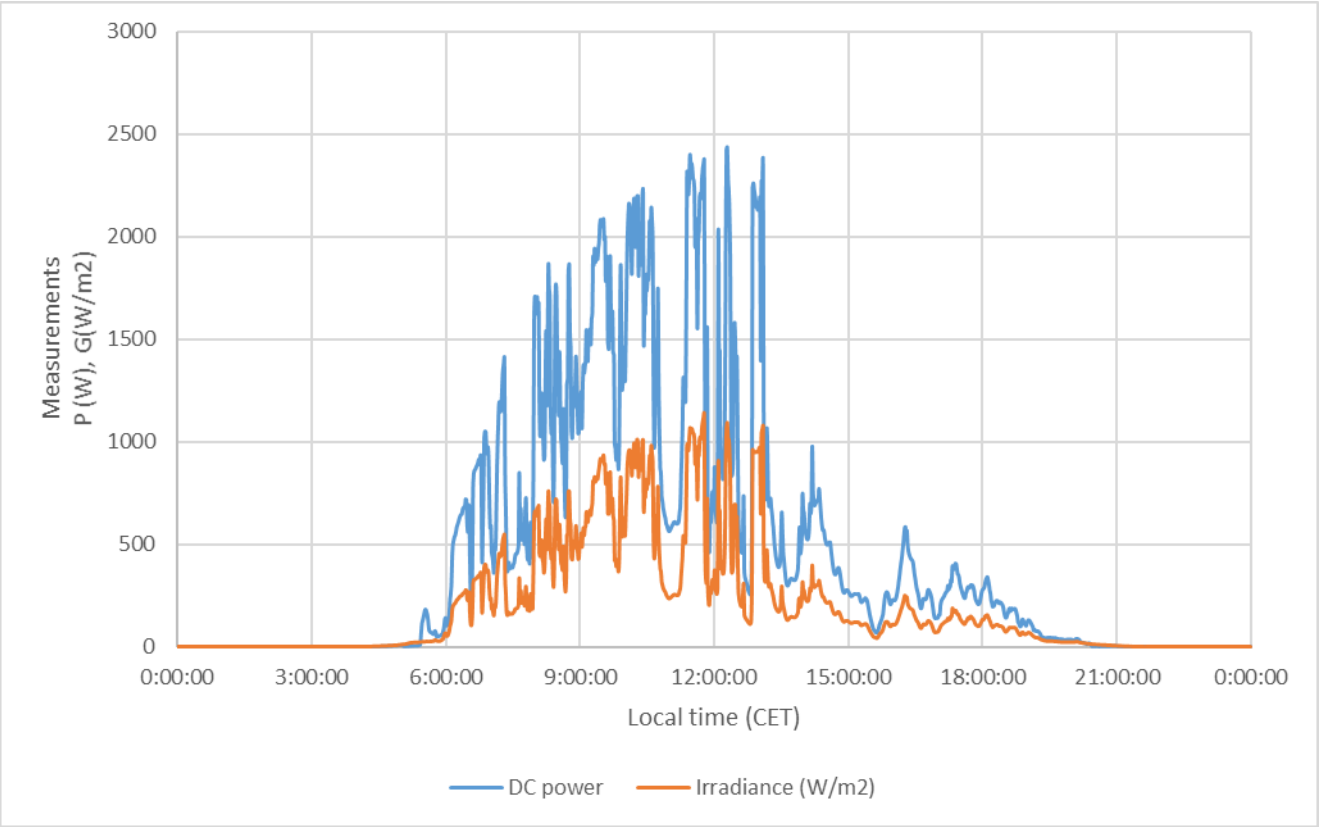

Figure 38: Solar irradiance and measured DC power, string 1. 6th of May.

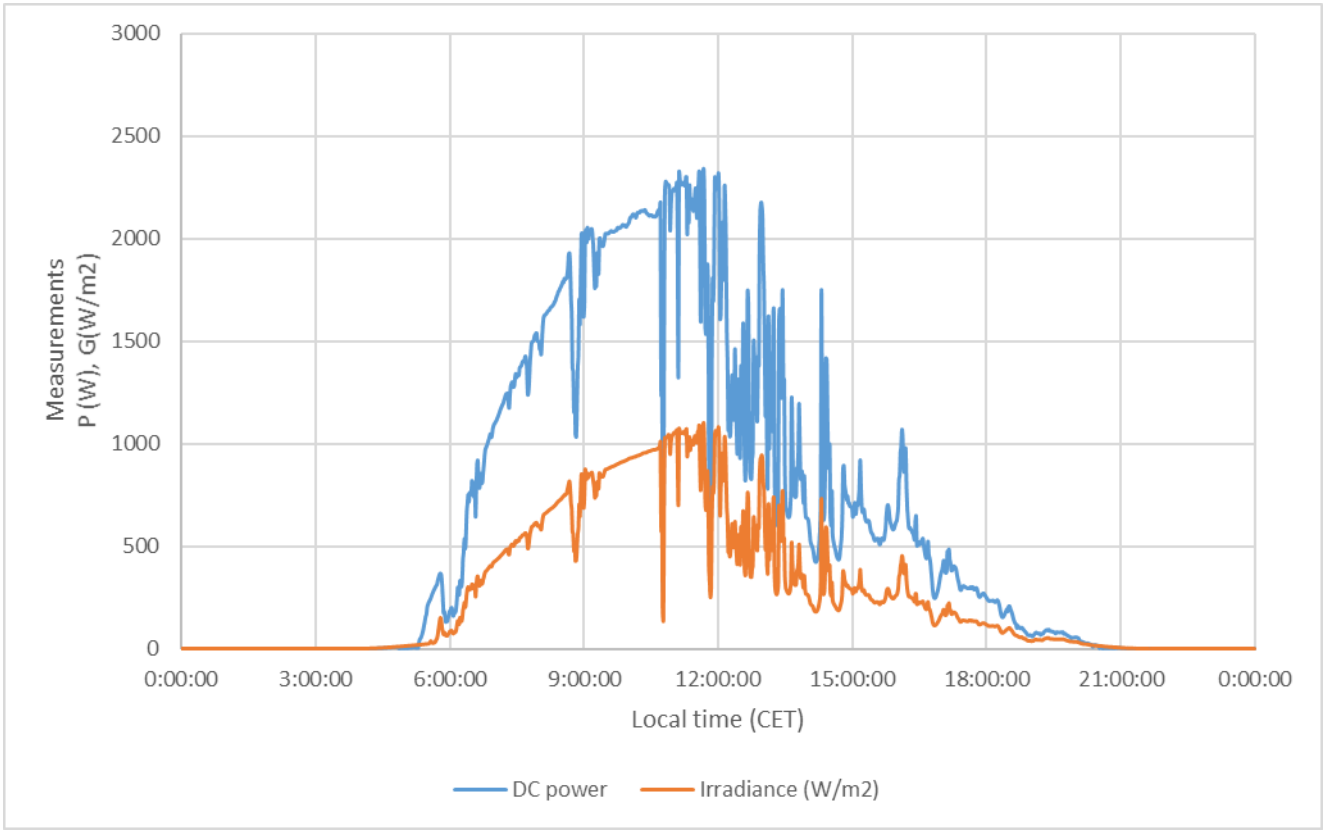

Figure 39: Solar irradiance and measured DC power, string 1. 7th of May.

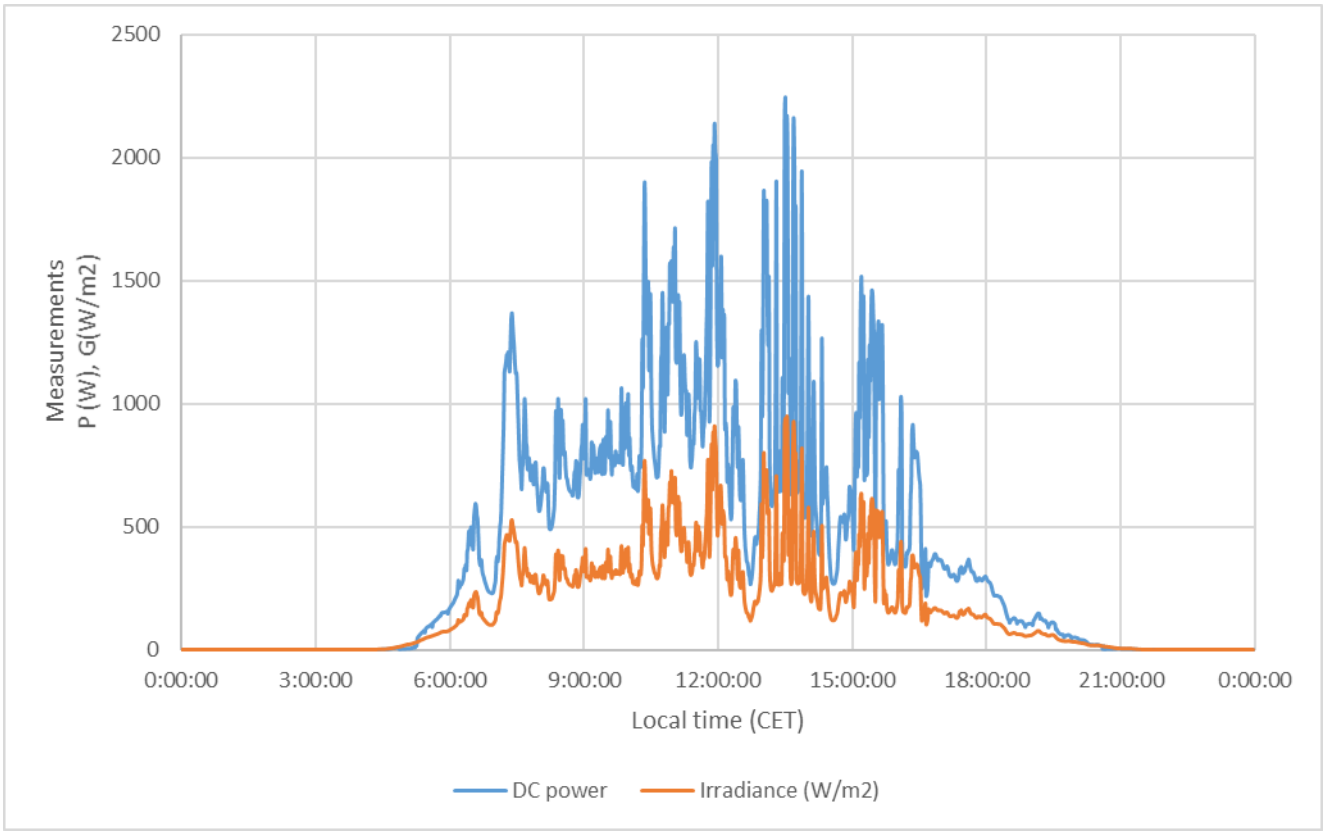

Figure 40 Solar irradiance and measured DC power, string 1. 8th of May

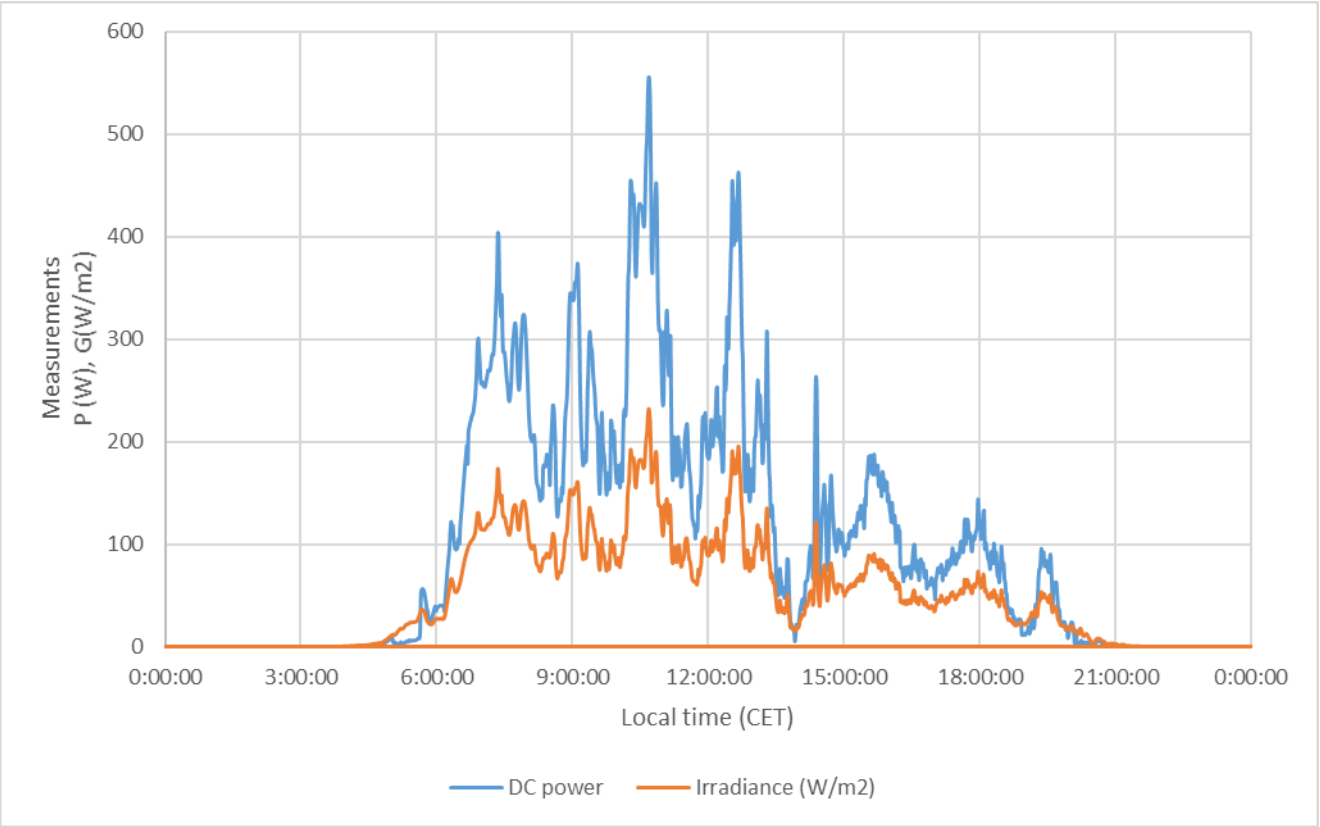

Figure 41: Solar irradiance and measured DC power, string 1. 10th of May

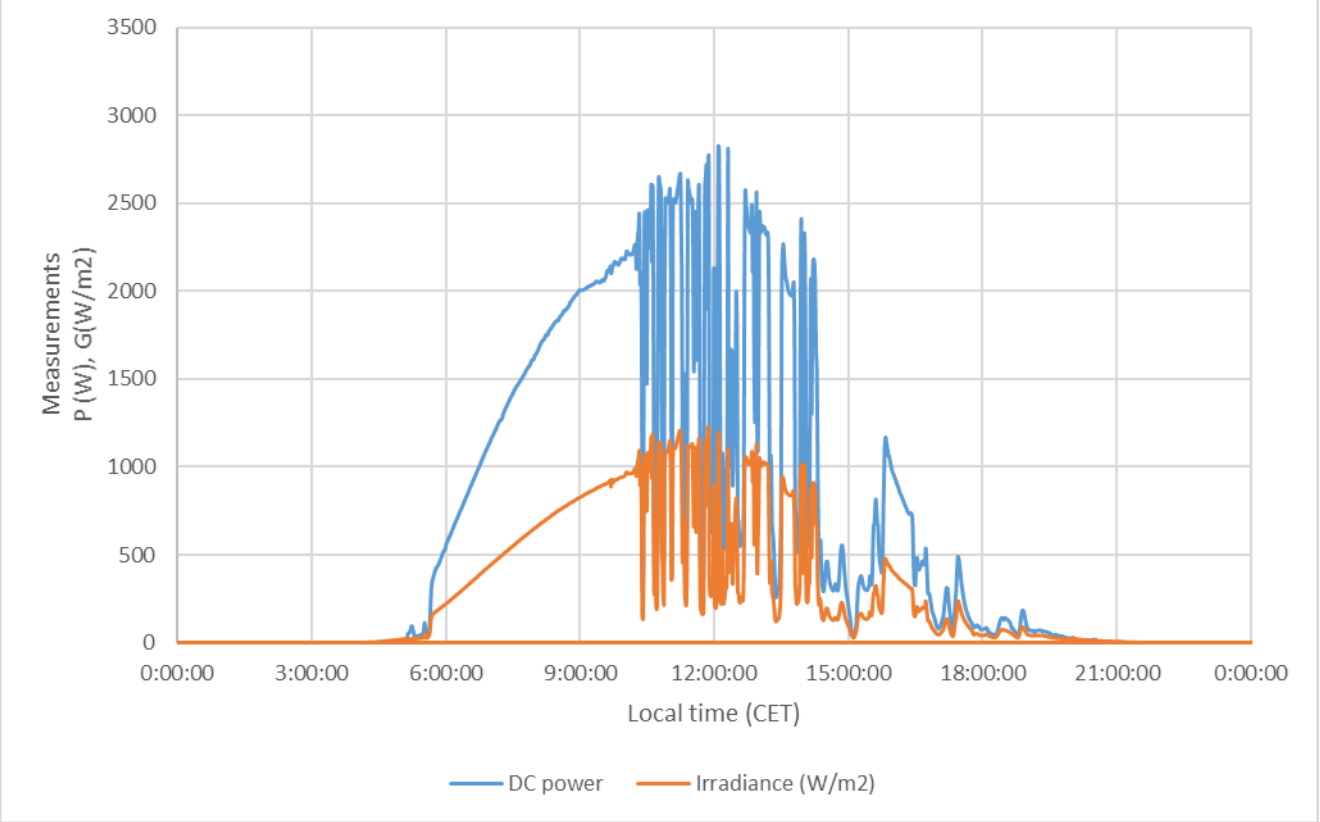

Figure 42: Solar irradiance and measured DC power, string 1. 11th of May

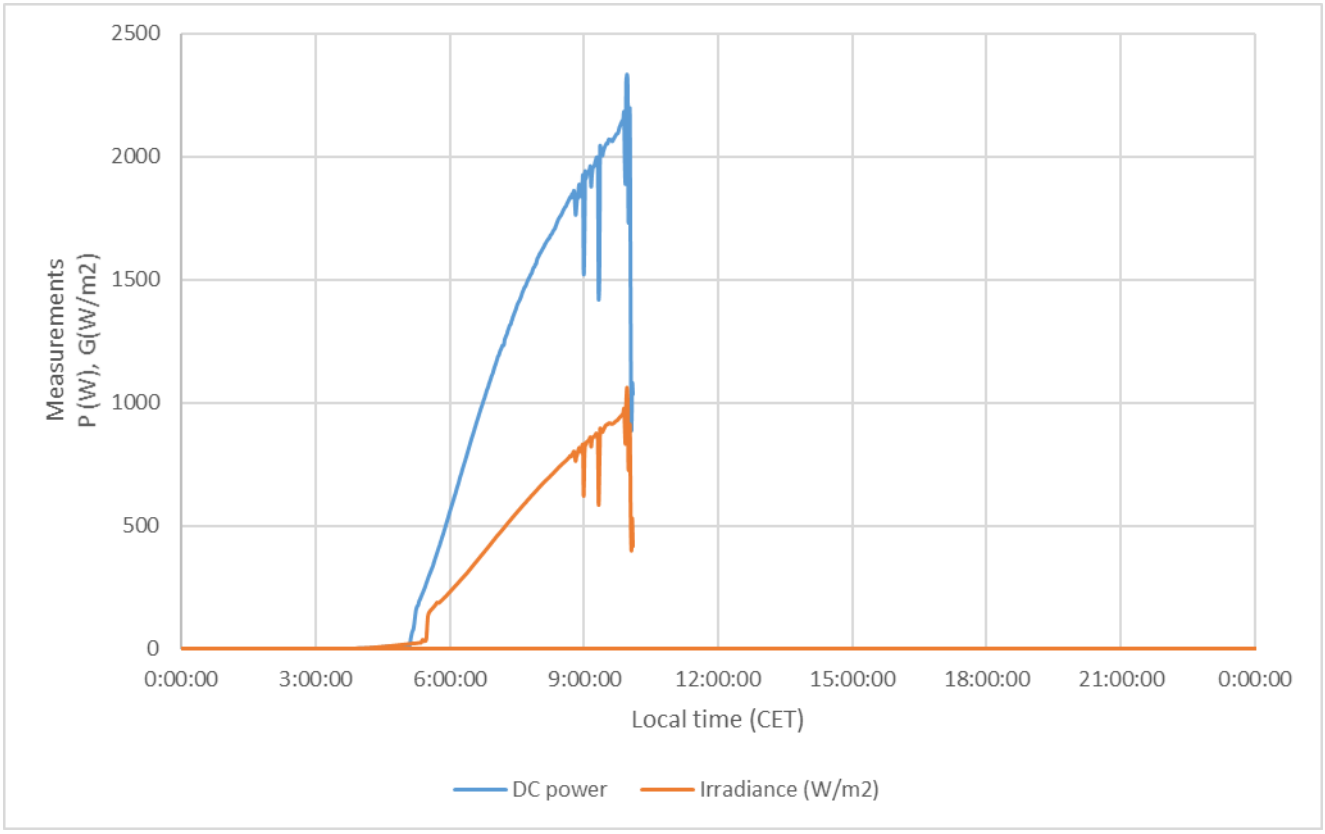

Figure 43 Solar irradiance and measured DC power, string 1. 12th of May

B. MEASURED POWER VS CORRECTED POWER

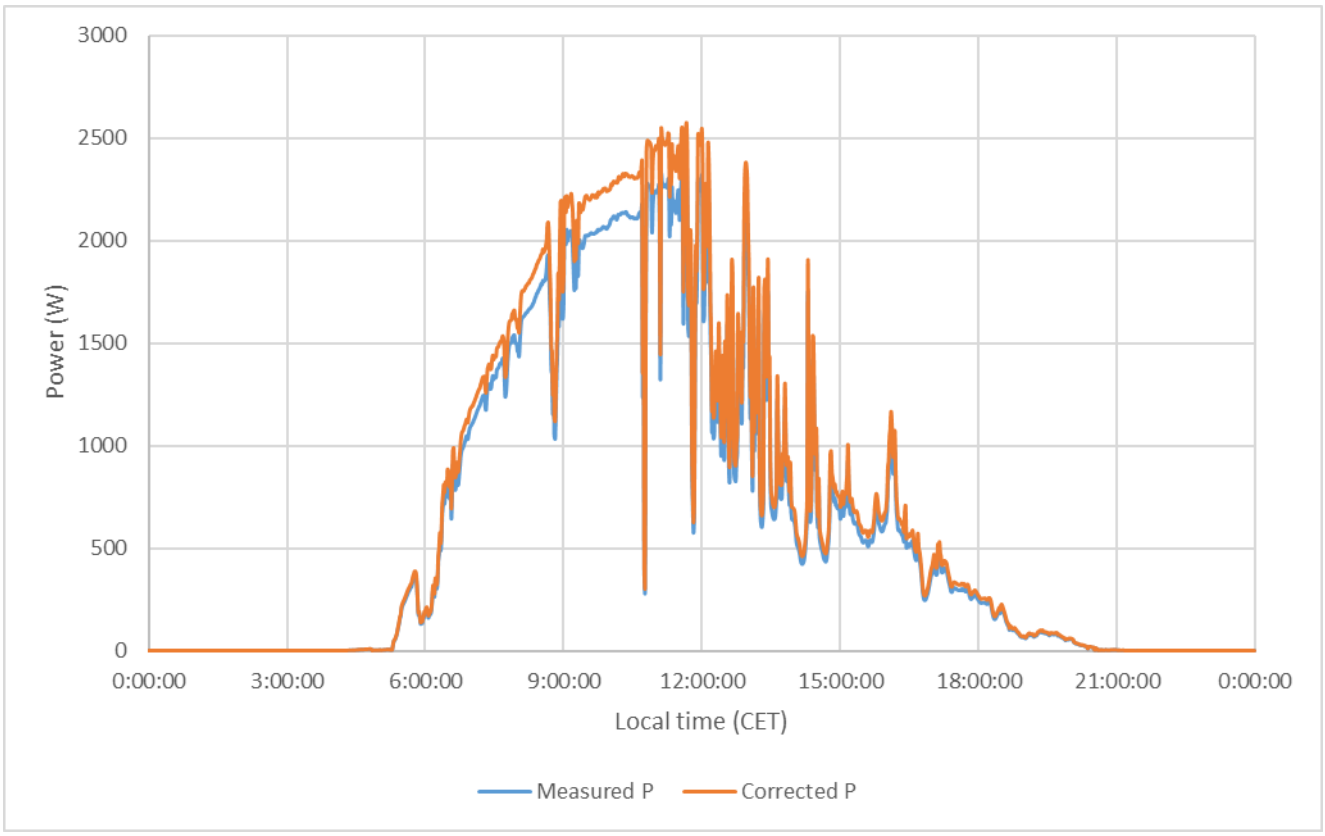

Figure 44: Measured power and corrected power in string 1. 7th of May.

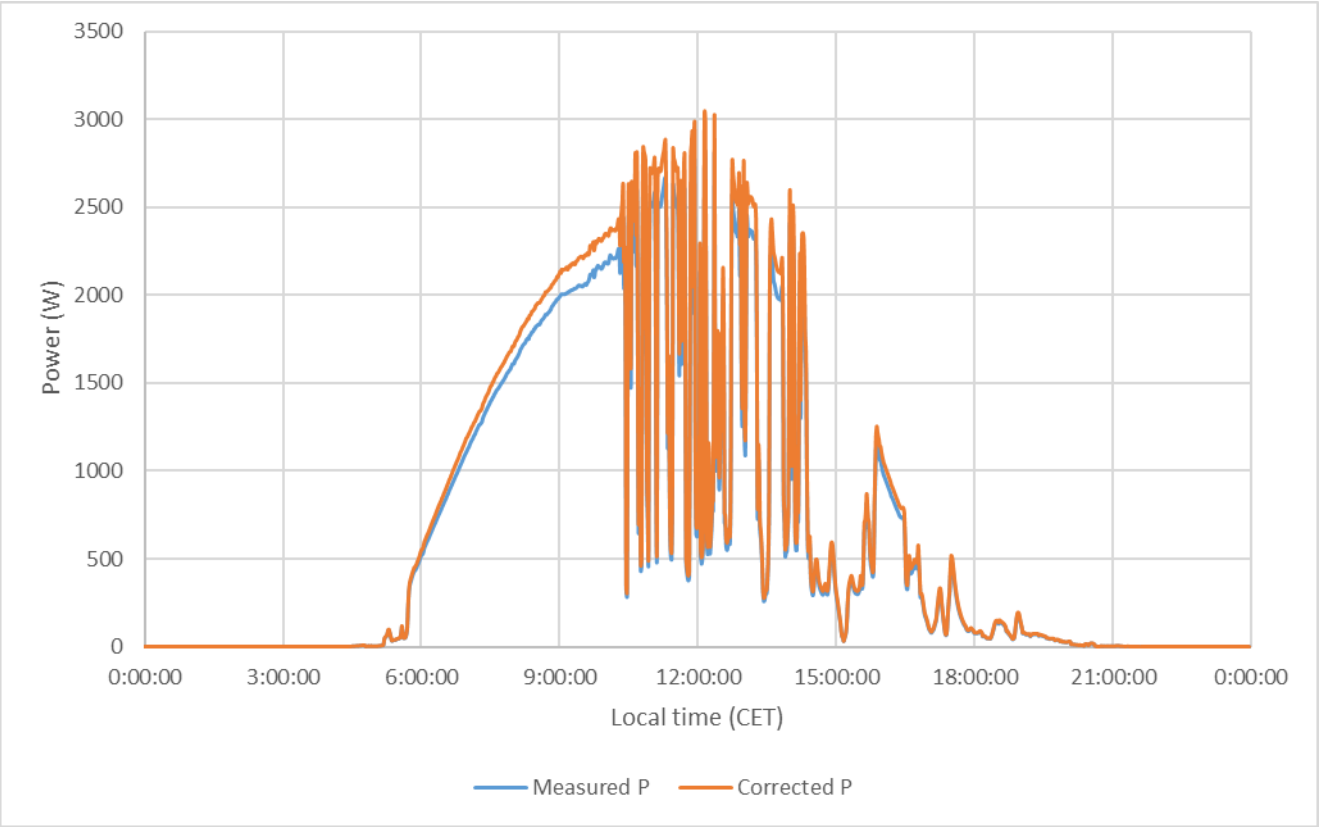

Figure 45: Measured power and corrected power in string 1. 11th of May.

APENDIX II: SPECIFICATIONS OF THE PV PLANT

A. ELECTRIC CONEXIONS OF THE PLAT

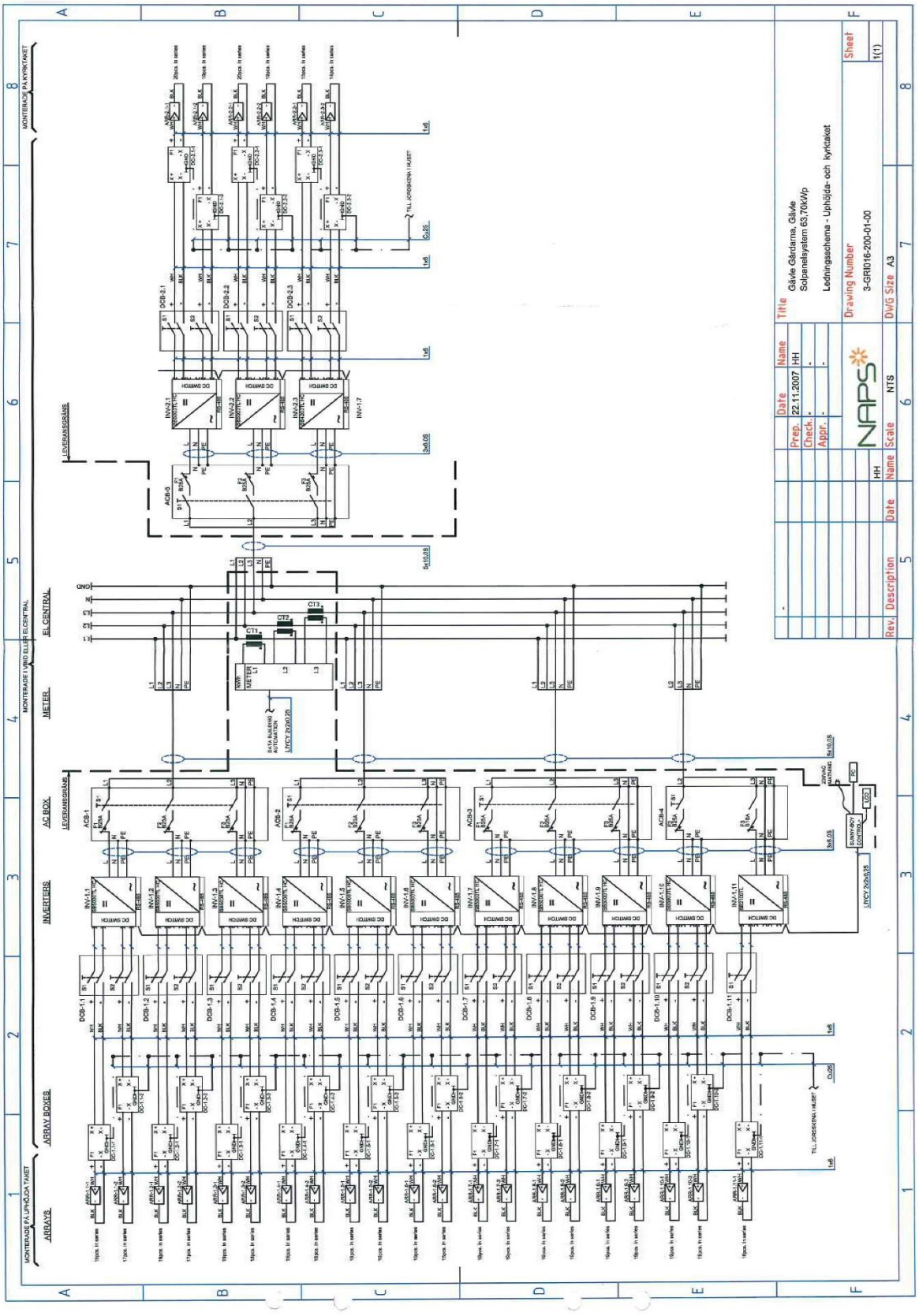

B. TECHNICAL DESCRIPTION OF THE PV MODULES

Technical Description

Photovoltaic Module NP130GK
Product Code: 13130, N00578

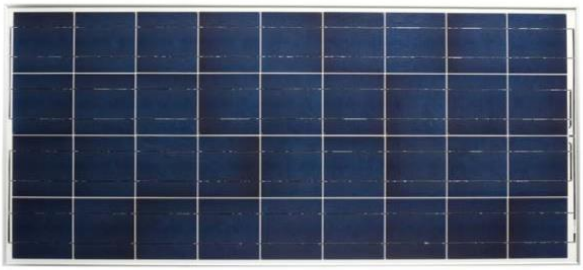

36 polycrystalline Si solar cells
Main application: general off-grid PV systems

Module Electrical Performance under Standard Test Conditions
Refers to standard test conditions of 1000 Wm $^{-2}$ solar irradiance, 25°C cell temperature, Air Mass 1.5.
Note: Maximum power point is subject to +5W/-0W variation. All other values are typical and for guidance only.
Maximum Power Point: 130 Watts, 7.68 Amps at 16.9 Volts.
Short Circuit: 8.45 Amps. Open circuit: 22.0 Volts.

Dimensions and Weight *all dimensions +/- 2mm, weight approximately +/-0.3kg*
Length: 1480mm. Width: 670mm. Thickness at edge: 34mm. Weight: 10.5kg

Construction
Top cover material: low iron tempered glass 3mm
Encapsulant (lamination material): EVA
2 factory-fitted bypass diodes
2 x 4mm earthing holes in frame
Rear cover material: Tedlar-Polyester-Tedlar white
Frame: anodised aluminium
1 junction box type S1410-2

Integral mounting holes
8 holes, size 7mm.
Along length: 740/1438mm centre to centre, 370/21mm centre to module edge.
Across width: 628/334mm centre to centre, 21/168mm centre to module edge.

Cell circuit
Cell dimensions: Length (tab direction) 156mm. Width: 156mm.
Electrical circuit: 36 cells in series
Cell layout: 4 rows, each row is 9 cells long.

Normal Operating Cell Temperature (NOCT)
47°C *error in measurement around +/- 2°C*
Cell temperature at 800Wm $^{-2}$ solar irradiance, 20°C ambient temperature, wind speed <=1ms $^{-1}$, free air access to rear.

Efficiencies based on Standard Test Conditions Rating
Module: 13.1% Laminated area: 13.3% Cells alone: 14.8%
Note: Standard Test Conditions efficiency figures should only be used to compare one module with another. These efficiency figures do not apply to actual field perfomance, for which a careful analysis of operating conditions is necessary to determine the effects of module temperature and other factors.

Specifications may change due to Naps policy of continuous product improvement.
Please check current specification before purchasing.
Information last updated: 26-Nov-10

Naps Systems Oy, Pakkalankuja 7A, FIN-01510 Vantaa, Finland
Tel +358 20 7545 666, Fax +358 20 7545 660, www.napssystems.com

C. STRINGS OF THE PLANT

NAPS

PROTOKOLL FÖR DRIFTSÄTTNING SOLCELLER
ANDERSBERGS CENTRUM, GAVLEGÅRDARNA

Datum: 2008-01-29
Uppgjord: 2008-01-29

Växelriktare	Ref	Serienummer	Inspänning MPP	Pos i SBC+	Paneler i serie R1	Paneler i serie R2
SB5000TL HC	INV-1.1	1100655340	125 - 750V	7	19	17
SB5000TL HC	INV-1.2	1100155528	125 - 750V	12	19	17
SB5000TL HC	INV-1.3	1100155349	125 - 750V	5	19	18
SB5000TL HC	INV-1.4	1100155372	125 - 750V	3	19	18
SB5000TL HC	INV-1.5	1100155367	125 - 750V	6	19	16
SB5000TL HC	INV-1.6	1100155532	125 - 750V	9	19	15
SB5000TL HC	INV-1.7	1100155397	125 - 750V	2	19	19
SB5000TL HC	INV-1.8	1100155344	125 - 750V	4	19	19
SB5000TL HC	INV-1.9	1100155400	125 - 750V	11	19	19
SB5000TL HC	INV-1.10	1100155398	125 - 750V	8	19	19
SB2100TL	INV-1.11	2000325080	125 - 600V	14	16	
SB5000TL HC	INV-2.1	1100155383	125 - 750V	1	20	19
SB5000TL HC	INV-2.2	1100155341	125 - 750V	13	20	19
SB4200TL HC	INV-2.3	1100155497	125 - 750V	10	15	14

Rader med 14 paneler i serie ger VOC	240 - 295
Rader med 15 paneler i serie ger VOC	255 - 315
Rader med 16 paneler i serie ger VOC	270 - 335
Rader med 17 paneler i serie ger VOC	290 - 360
Rader med 18 paneler i serie ger VOC	305 - 380
Rader med 19 paneler i serie ger VOC	320 - 400
Rader med 20 paneler i serie ger VOC	340 - 420

Mätning av VOC och polaritet
Kontrollera att brytare i DC-Box och AC-box är frånslagna.
Öppna DC-Box och mät VOC och kontrollera polaritet.

	DC-Box	VOC	Tid	Polaritet	Kommentar
DCB-1.1	S1	410	11.00	OK	OK
	S2	410	11.00	OK	OK
	DC-Box	VOC	Tid	Polaritet	Kommentar
DCB-1.2	S1	405	11.00		
	S2	364	11.00		
	DC-Box		Tid	Polaritet	Kommentar
DCB-1.3	S1	407	11.00	OK	
	S2	407	11.00	OK	
	DC-Box	VOC	Tid	Polaritet	Kommentar
DCB-1.4	S1	321	11.00	OK	1)
	S2	407	11.00	OK	
	DC-Box	VOC	Tid	Polaritet	Kommentar
DCB-1.5	S1	405	11.10	OK	
	S2	404	11.10	OK	
	DC-Box	VOC	Tid	Polaritet	Kommentar
DCB-1.6	S1	403	11.10	OK	
	S2	409	11.10	OK	

Naps Sweden AB
Box 26
127 21 Skärholmen

1(3)

D. PLANT DESCRIPTION

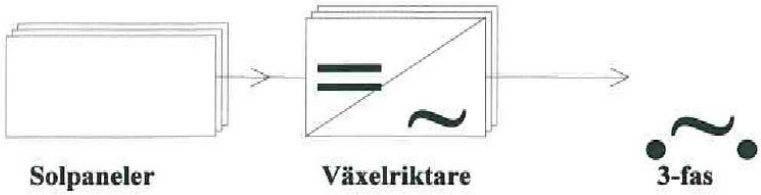

Blockschema solenergianläggning

Systemfakta	
Nominell effekt/solpanel	130W(*)
Typ av solpanel	NP130GK med polykristallina solceller
Antal solpaneler	490
Total yta solpaneler:	486 m²
Nominell max. effekt DC:	63,7 kW(*)
Nominell max. effekt AC:	66,3 kW
Nominell spänning AC:	230VAC
Solpanelerna är monterade på tråg infästa på det platta taket samt i ett profilsystem på det triangulära taket	
(*) Gäller vid solinstrålning 1000W/m², 25°C	

1 Beskrivning av systemets huvudkomponenter

Solpaneler

En solcell är en högteknologisk produkt som utnyttjar den fotovoltaiska effekten för att producera elström (eng, photovoltaic PV). Solcellen omvandlar ljuset direkt utan några rörliga delar, till elektrisk energi. Det finns två huvudtyper av solceller. Monokristallina och polykristallina. Skillnaden är tillverkningsmetoden. För monokristallint kisel låter man staven, som sedan sågas till celler, långsamt växa från en smälta och det bildas då en enda kiselkristall. I den andra metoden häller man smältan i en gjutform och låter den svalna under kontrollerade former. Det bildas då fler kiselkristaller och kallas polykristallint kisel. Monokristallina celler har normalt något bättre verkningsgrad men skillnaden är inte så stor idag jämfört med 10-15 år sedan. Huvuddelen av världsproduktionen består av polykristallina solpaneler som kostar något mindre att tillverka. En solcell består av en tunn skiva kisel med kontakter på fram- och baksidan. Om solcellen exponeras för ljus uppstår en spänning mellan fram- och baksida, Ansluter man kontakterna till någon förbrukare får man en elektrisk ström. Solpanelerna har 36 solceller kopplade i serie och har en nominell spänning av 12 VDC.